

NPS ARCHIVE
1965
LUNDBERG, D.

**LAMINAR CONVECTIVE HEAT TRANSFER
IN THE ENTRANCE REGION BETWEEN
PARALLEL FLAT PLATES**

D. D. LUNDBERG

DUDLEY KNOX LIBRARY
NAVAL POSTGRADUATE SCHOOL
MONTEREY CA 93943-5101

LAMINAR CONVECTIVE HEAT TRANSFER
IN THE ENTRANCE REGION BETWEEN PARALLEL FLAT PLATES

* * * * *

D. D. Lundberg

LAMINAR CONVECTIVE HEAT TRANSFER
IN THE ENTRANCE REGION BETWEEN PARALLEL FLAT PLATES

by

D. D. Lundberg

Captain, United States Marine Corps

Submitted in partial fulfillment of
the requirements for the degree of

MASTER OF SCIENCE
IN
AERONAUTICAL ENGINEERING

United States Naval Postgraduate School
Monterey, California

1 9 6 5

NPS ARCHIVE
1965
LUNDBERG, D.

~~SECRET~~
C.I.

LAMINAR CONVECTIVE HEAT TRANSFER
IN THE ENTRANCE REGION BETWEEN PARALLEL FLAT PLATES

by

D. D. Lundberg

This work is accepted as fulfilling
the thesis requirements for the degree of

MASTER OF SCIENCE

IN

AERONAUTICAL ENGINEERING

from the

United States Naval Postgraduate School

ACKNOWLEDGEMENT

The author wishes to express his gratitude to Dr. James A. Miller, Associate Professor, Department of Aeronautical Engineering, for his assistance, and interest. Dr. Miller suggested the project and provided his paper on the subject, which proved to be a valuable reference. In addition, Professor Miller's excellent lectures on boundary layer theory, and heat and mass transfer were found to be highly informative and stimulating.

ABSTRACT

Heat transfer rates for laminar, convective heat transfer in the entrance region between parallel plates are investigated. The hydrodynamic solution due to Bodia $\overline{[2]}$ was used in the solution of the energy equation in finite difference form on a digital computer. The thermal boundary conditions include: constant heat input, constant wall temperature, one wall constant temperature and one wall insulated, and constant but different wall temperatures on the upper and lower walls.

The approximate, integral methods of Siegel and Sparrow $\overline{[5]}$, $\overline{[7]}$ produce results that are in close agreement with the solutions in this analysis for the constant heat input and constant wall temperature cases.

The scope of the finite difference solution is limited to a narrow range of Prandtl numbers near unity, due to the small grid sizes required for convergence at small Prandtl numbers and to the overly low transfer rates indicated near the entrance for high Prandtl numbers, which is a result of the "finite starting length."

TABLE OF CONTENTS

	Page
I. Introduction	1
II. Analysis	3
A. Governing Equations	3
B. Hydrodynamic Solution	5
C. Energy Solution	6
D. Thermal Boundary Conditions in Finite Difference Form	10
E. Computational Procedures	12
III. Results	14
IV. Conclusion	19
References	20
Tables	21
Illustrations	27
Appendix	59

LIST OF TABLES

Table		Page
I	Local Nusselt Numbers for Constant Heat Input PR = 0.7	21
II	Local Nusselt Numbers for Constant Wall Temperature (Symmetric Case) PR = 0.7	22
III	Local Nusselt Numbers for one Wall Constant Temperature, One Wall Insulated PR = 0.7	23
IV	Dimensionless Heat Flux for Constant Wall Temperature (Asymmetric Case) $\frac{N_1 - 1}{N_2 - 1} = 1/2$ PR = 0.7	24
V	Dimensionless Heat Flux for Constant Wall Temperature (Asymmetric Case) $\frac{N_1 - 1}{N_2 - 1} = 1/3$ PR = 0.7	25
VI	Dimensionless Heat Flux for Constant Wall Temperature (Asymmetric Case) $\frac{N_1 - 1}{N_2 - 1} = 1/4$ PR = 0.7	26

LIST OF ILLUSTRATIONS

Figure		Page
1a.	Designation of Mesh Points	27
1b.	Axis System, Symmetric Cases	27
1c.	Axis System, Asymmetric Cases	27
2.	Comparison of Dimensionless Pressure Decrements due to Bodoia, Schlichting and Han	28
3.	Comparison of Velocity Distribution due to Bodoia and Schlichting	29
4.	Comparison of Velocity Distribution due to Bodoia and Schiller	30
5.	Comparison of Local Nusselt Numbers Constant Heat Input	31
6.	Local Nusselt Numbers Constant Heat Input for PR = 0.5, 0.7, 1.0, 1.6, 3.2, 10	32
7.	Temperature and Velocity Profiles Constant Heat Input X = .005	33
8.	Temperature and Velocity Profiles Constant Heat Input X = .050	34
9.	Temperature and Velocity Profiles Constant Heat Input X = .250	35
10.	Temperature and Velocity Profiles Constant Heat Input X = 1.000	36

Figure		Page
11.	Comparison of Local Nusselt Numbers Constant Wall Temperature (Symmetric Case)	37
12.	Local Nusselt Numbers Constant Wall Temperatures (Symmetric Case) PR = 0.5, 0.7, 1.0, 1.6, 3.2, 10	38
13.	Temperature and Velocity Profiles Constant Wall Temperature (Symmetric Case) X = .005	39
14.	Temperature and Velocity Profiles Constant Wall Temperature (Symmetric Case) X = .050	40
15.	Temperature and Velocity Profiles Constant Wall Temperature (Symmetric Case) X = .250	41
16.	Temperature and Velocity Profiles Constant Wall Temperature (Symmetric Case) X = 1.000	42
17.	Local Nusselt Numbers One Wall Constant Temperature One Wall Insulated PR = 0.5, 0.7, 1.0, 1.6, 3.2, 10.	43
18.	Temperature and Velocity Profiles One Wall Constant Temperature One Wall Insulated X = .005	44
19.	Temperature and Velocity Profiles One Wall Constant Temperature One Wall Insulated X = .050	45

Figure		Page
20.	Temperature and Velocity Profiles One Wall Constant Temperature One Wall Insulated X = .250	46
21.	Temperature and Velocity Profiles One Wall Constant Temperature One Wall Insulated X = 1.000	47
22a.	Dimensionless Heat Flux Constant Wall Temperature (Asymmetric Case) $\frac{N_1 - 1}{N_2 - 1} = 1/2$ PR = 0.5, 0.7, 1.0	48
22b.	Dimensionless Heat Flux Constant Wall Temperature (Asymmetric Case) $\frac{N_1 - 1}{N_2 - 1} = 1/2$ PR = 1.6, 3.2, 10.	49
23a.	Dimensionless Heat Flux Constant Wall Temperature (Asymmetric Case) $\frac{N_1 - 1}{N_2 - 1} = 1/3$ PR = 0.5, 0.7, 1.0	50
23b.	Dimensionless Heat Flux Constant Wall Temperature (Asymmetric Case) $\frac{N_1 - 1}{N_2 - 1} = 1/3$ PR = 1.6, 3.2, 10	51
24a.	Dimensionless Heat Flux Constant Wall Temperature (Asymmetric Case) $\frac{N_1 - 1}{N_2 - 1} = 1/4$ PR = 0.5, 0.7, 1.0	52

Figure		Page
24b.	Dimensionless Heat Flux Constant Wall Temperature (Asymmetric Case) $\frac{N_1 - 1}{N_2 - 1} = 1/4$ PR = 1.6, 3.2, 10	53
25.	Temperature and Velocity Profiles Constant Wall Temperature (Asymmetric Case) X = .005	54
26.	Temperature and Velocity Profiles Constant Wall Temperature (Asymmetric Case) X = .050	55
27.	Temperature and Velocity Profiles Constant Wall Temperature (Asymmetric Case) X = .250	56
28.	Temperature and Velocity Profiles Constant Wall Temperature (Asymmetric Case) X = 1.000	57
29.	Local Nusselt Number Constant Wall Temperature (Asymmetric Case) $\frac{N_1 - 1}{N_2 - 1} = 1/4$ PR = 0.7	58

TABLE OF SYMBOLS

English Letter Symbols

c	Specific heat
d	Half the distance of separation of the parallel flat plates
D	Hydraulic diameter $D = 4d$
h	Unit conductance for convection heat transfer
k	Unit thermal conductivity
L	Dimensionless length parameter, $\frac{x/D}{Re_D} = \frac{X}{16}$
q"	Heat flux per unit area, q/A
q*	Dimensionless heat flux, $\frac{qD}{Akt_o}$
t	Temperature
t_o	Initial fluid temperature
t_m	Mixed mean temperature
t_w	Wall temperature
t_{w1}	Lower wall temperature (asymmetric case)
t_{w2}	Upper wall temperature (asymmetric case)
T	Dimensionless temperature, t/t_o
T_w	Dimensionless wall temperature, t_w/t_1
T_m	Dimensionless mixed mean temperature, t_m/t_o
u	Axial velocity component

u_0	Initial axial velocity component
U	Dimensionless axial velocity, u/u_0
v	Crosswise velocity component
v_c	Crosswise velocity component at centerline
v_0	Initial crosswise velocity component
V	Dimensionless crosswise velocity component, v/v_0
X	Dimensionless length parameter, $\frac{\nu x}{d^2 u_0}$
y	Normal coordinate
Y	Dimensionless normal coordinate, y/d

Greek Letter Symbols

ρ	Fluid density
μ	Fluid viscosity
ν	Kinematic viscosity, μ/ρ

Non-dimensional Groups

N_{u_x}	Local Nusselt number, $\frac{hD}{k}$
PR	Prandtl number, $\frac{\mu c_p}{k}$
Re_d	Reynolds number, based on half the gap width, $\frac{du_0}{\nu}$
Re_D	Reynolds number, based on hydraulic diameter, $\frac{Du_0}{\nu}$

I. INTRODUCTION

Efficient design of compact heat exchangers such as are employed for gas turbine regenerators, among other applications, requires maximum utilization of the high transfer rates available in the entrance region. In this region the velocity and temperature profiles of the entering fluid are undergoing rapid transition from their uniform distribution at entrance to the fully established distributions encountered farther downstream. The well known Graetz solution, in which only the temperature development is considered, does not yield adequate results when the velocity and temperature distributions are simultaneously developing. This is particularly true if the entrance region represents a considerable percentage of overall length and the two profiles develop at approximately the same rates. This situation is frequently encountered with gases where the Prandtl number is approximately one.

The purpose of the present analysis is to present a finite difference solution for the heat transfer rates between parallel flat plates for several different boundary conditions corresponding to various constant wall temperatures and constant heat input configurations. The approach to the problem was suggested by Miller $\overline{1}$, which is adapted from the numerical procedures applied to the entrance region of the circular tubes by Kays $\overline{2}$.

While an analysis such as the present one can hardly compete for simplicity with approximate treatments such as the Graetz analysis, or the several energy integral analyses commonly employed in engineering design, it does provide an exact solution for a limited number of cases which serves as a standard with which the accuracy of the various approximate methods may be assessed.

II. ANALYSIS

A. Governing Equations

The governing equations are the energy, momentum (Navier-Stokes) and continuity equations. In order to reduce the complexity and coupling of the equations, the following assumptions are made.

The flow is assumed to be:

1. steady, two-dimensional
2. laminar
3. incompressible

In addition it is assumed that:

1. thermal diffusivity (α) is constant
2. convective heat transfer is large compared to radiation, axial conduction, and viscous dissipation.

The governing equations in reduced form may then be expressed as:

Energy:

$$u \frac{\partial t}{\partial x} + v \frac{\partial t}{\partial y} = \alpha \frac{\partial^2 t}{\partial y^2} \quad (1)$$

Momentum:

$$u \frac{\partial u}{\partial x} + v \frac{\partial u}{\partial y} = -\frac{1}{\rho} \frac{\partial p}{\partial x} + \nu \frac{\partial^2 u}{\partial y^2} \quad (2)$$

Continuity:

$$\frac{\partial u}{\partial x} + \frac{\partial v}{\partial y} = 0 \quad (3)$$

Due to the assumption of incompressibility the above equations are no longer coupled. The temperature development remains dependent upon the velocity profile, although dependence of velocity on temperature has been removed.

The boundary conditions associated with equations (1), (2), and (3) for flow between parallel flat plates with uniform velocity and temperature at entrance are:

1. At the entrance ($x = 0$)

$$t = t_o = C_1$$

$$u = u_o = C_2$$

$$v = v_o = 0$$

2. At the walls ($y = \pm d$)

$$v = v_w = 0$$

$$u = u_w = 0$$

$$t = t_w$$

3. On centerline

$$v = v_c = 0$$

4. Applied thermal boundary conditions

(1) symmetric cases (with respect to duct centerline)

a. constant wall temperature

$$t_w = C_3$$

b. constant heat input

$$\left(\frac{\partial t_w}{\partial y}\right)_{y=0} = C_4$$

(2) asymmetric cases

a. one wall constant temperature, one wall insulated

$$t_{w_1} = C_5$$

$$\left(\frac{\partial t_{w_2}}{\partial y}\right)_{y=0} = 0$$

b. constant wall temperature

$$t_{w_1} = C_6$$

$$t_{w_2} = C_7$$

where: $C_6 \neq C_7$

Solution of the energy equation requires that a hydrodynamic solution be first obtained.

B. Hydrodynamic Solution

Several hydrodynamic solutions for the entrance region are available. Solutions have been presented by Bodoia [3], Schlichting [4], Schiller [5], and Han [6]. The approximate solutions of Schiller and Han have the advantage of being analytic, and therefore, less cumbersome to use. They are, however, inherently less accurate than the numerical solutions presented by Bodoia and Schlichting.

Bodoia's solution was obtained by evaluation of the Prandtl boundary layer equations in finite-difference form. Velocity profiles were obtained at given streamwise locations by utilizing matrix methods to simultaneously solve a column array of momentum expressions normal to the flow.

A comparison of Schlichting's series solution and the Bodoia solution indicates that, in addition to the velocity gradient discontinuity in the Schlichting solution where the upstream and downstream solutions are joined, Schlichting's representation of the pressure gradient, based only on the centerline velocity, results in a core velocity gradient which is too large and a wall velocity gradient which is too small $\sqrt{3}$.

Comparisons of the dimensionless pressure decrement versus length due to Bodoia, Schlichting and Han are presented in Fig. 2. Velocity distribution comparisons between Bodoia and Schlichting, and Schlichting and Schiller, are shown in Figs. 3 and 4.

The Bodoia solution was adopted for the present analysis.

C. Energy Solution

Equations (1) and (3) may be written in dimensionless form by introducing the following dimensionless variables:

$$\begin{array}{lll}
 T = t/t_0 & X = \frac{\nu x}{d^2 u_0} = \frac{x/d}{Re} & U = u/u_0 \\
 Y = y/d & & V = v/u_0
 \end{array}$$

In dimensionless form, the equations are then:

Energy:

$$U \frac{\partial T}{\partial X} + Re V \frac{\partial T}{\partial Y} = \frac{1}{PR} \frac{\partial^2 T}{\partial Y^2} \quad (4)$$

Continuity:

$$\frac{\partial U}{\partial X} + Re \frac{\partial V}{\partial Y} = 0 \quad (5)$$

The following finite difference approximations are then introduced:

$$\frac{\partial T}{\partial X} = \frac{\Delta T}{\Delta X} = \frac{T_{x+1,y} - T_{x,y}}{\Delta X} \quad (6)$$

$$\frac{\partial T}{\partial Y} = \frac{\Delta T}{\Delta Y} = \frac{T_{x,y+1} - T_{x,y-1}}{2 \Delta Y} \quad (7)$$

$$\frac{\partial^2 T}{\partial X^2} = \frac{T_{x,y+1} - 2T_{x,y} + T_{x,y-1}}{\Delta Y^2} \quad (8)$$

$$\frac{\partial U}{\partial X} = \frac{\Delta U}{\Delta X} = \frac{U_{x+1,y} - U_{x-1,y}}{2 \Delta X} \quad (9)$$

$$\frac{\partial V}{\partial Y} = \frac{\Delta V}{\Delta Y} = \frac{V_{x,y} - V_{x,y-1}}{\Delta Y} \quad (10)$$

Note that (6) is a forward difference and (10) is a backward difference, whereas the remaining equations are of the central difference

type. These have been expressed in this manner for simplicity and convenience. The larger truncation error normally associated with the forward or backward difference is not significant here since practical grid dimensions require that:

$$\Delta Y \gg \Delta X$$

and, due to the nature of the flow:

$$\frac{\Delta U}{\Delta X} \gg \frac{\Delta V}{\Delta Y}$$

Introducing (6) through (10) into (4) and (5) and solving for the appropriate term yields:

$$\begin{aligned} T_{x+1,y} = & \left[\frac{\Delta X}{U P R \Delta Y^2} + \frac{\Delta X Re V}{U^2 \Delta Y} \right] T_{x,y-1} + \\ & \left[1 - \frac{2 \Delta X}{U P R \Delta Y^2} \right] T_{x,y+1} + \\ & \left[\frac{\Delta X}{U P R \Delta Y^2} - \frac{\Delta X Re V}{U^2 \Delta Y} \right] T_{x,y+1} \end{aligned} \quad (11)$$

$$V_{x,y} = V_{x,y-1} + \frac{\Delta Y}{Re^2 \Delta X} \left[U_{x-1,y} - U_{x+1,y} \right] \quad (12)$$

which constitute the computing equations.

Note that the Reynolds number (Re), although appearing in the above equations, remains only for convenience and could be eliminated. It is no longer a parameter in the set of equations having been included in the dimensionless length variable (X).

A mixed mean temperature (t_m) may be expressed in the following way:

$$t_m = \frac{\int c_p \rho u t \, dA}{\int c_p \rho u \, dA} \quad (13)$$

Removing the constants from within the integral, and simplifying, a dimensionless mixed mean temperature may be written in finite difference form:

$$T_m = \frac{\sum_{Y=0}^{Y=1} U_{x,Y} T_{x,Y}}{\sum_{Y=0}^{Y=1} U_{x,Y}} \quad (14)$$

Due to the no-slip condition imposed upon viscous flows, heat transfer to or from the fluid at the wall may be expressed in terms of conduction through a thin film of stagnant fluid. Thus:

$$q'' = q/A = k \left(\frac{\partial t}{\partial y} \right)_{y=0} \quad (15)$$

which must equal the heat flux due to convection,

$$q'' = q/A = h(t_w - t_m) \quad (16)$$

Defining the local Nusselt number as;

$$Nu_x = \frac{hd}{k} \quad (17)$$

Combining (14) and (15),

$$Nu_x = \frac{\left(\frac{\partial t}{\partial y} \right)_{y=0}}{t_w - t_m} \quad (18)$$

A Nusselt number based on the hydraulic diameter (d) instead of half the gap width (d) in finite difference form becomes;

$$N_{u_x} = \frac{4(T_w - T_{w-\Delta Y})}{\Delta Y} \frac{1}{T_w - T_m} \quad (19)$$

The hydraulic diameter was introduced in (19) to enable comparisons with previous solutions. The conversion is:

$$D = 4d$$

In addition, for the asymmetric constant wall temperature case, it is convenient to use a dimensionless parameter other than the Nusselt number. A dimensionless heat flux parameter may be defined by using (15) above:

$$\begin{aligned} q_f^* &= \frac{qD}{Akt_0} = \frac{D}{kt_0} \left[h \left(\frac{\partial t}{\partial y} \right)_{y=0} \right] \\ &= \frac{D}{kt_0} \left[\frac{kt_0}{d} \left(\frac{\partial T}{\partial Y} \right)_{Y=0} \right] \\ &= 4 \left(\frac{\partial T}{\partial Y} \right)_{Y=0} \end{aligned}$$

D. Thermal Boundary Conditions In Finite Difference Form

Constant Wall Temperature (Symmetric Case) Since the temperature distribution is symmetrical with respect to the centerline, computations were performed in only the upper half of the duct. A coordinate system was adapted with the X axis on the centerline of the channel. The thermal boundary condition at the wall was applied as:

$$t_w/t_o = T_w = N$$

where N is a positive integer.

Constant Heat Input (Symmetric Case) With the axis system as above, the slope of the thermal profile was maintained constant at the wall by adding a constant to the calculated temperature one step from the wall, thus:

$$T_w = T_w - \Delta y + M$$

where: $M = (\Delta T / \Delta Y)_w \cdot \Delta Y$

Constant Wall Temperature with One Wall Insulated. For this case the coordinate system was redefined so the X axis coincided with the lower wall. The lower wall boundary condition was taken to be:

$$t_{w1}/t_o = T_{w1} = N$$

while zero slope at the upper wall was obtained by equating the wall temperature to the calculated temperature one step from the wall:

$$t_{w2}/t_o = T_{w2} = T_{w2} - \Delta Y$$

Constant Wall Temperature (Asymmetric Case). With the axis system the same as for the insulated wall case, thermal boundary conditions were established as;

$$t_{w1}/t_o = T_{w1} = N_1$$

$$t_{w2}/t_o = T_{w2} = N_2$$

where N_1 and N_2 are positive integers and $N_1 \neq N_2$.

Noting that:

$$\frac{t_{w1} - t_o}{t_{w2} - t_o} = \frac{t_{w1}/t_o - 1}{t_{w2}/t_o - 1} = \frac{N_1 - 1}{N_2 - 1}$$

Values of $N_1 - 1 / N_2 - 1$ of 1/2, 1/3, 1/4 were investigated.

E. Computational Procedure

The finite difference solution was obtained by using a CDC 1604 digital computer to solve the equations at intervals of $\Delta X = 0.001$ and $\Delta Y = 0.1$. Velocity distributions were obtained by interpolating plotted curves of Bodoia's tabulated results.

Since the entire solution is dependent upon the first calculations at the entrance, starting values were obtained by reducing the grid size to $\Delta X = 0.0001$ and $\Delta Y = 0.05$ for the first 20 streamwise stations from $X = 0$ to 0.0020.

The continuity equation (2) was evaluated and the cross-wise velocity component (V) was introduced into the energy equation (11) at each grid point. The energy solution was then obtained at intervals of Y between centerline and the wall at each streamwise station.

Solutions for each thermal boundary condition were obtained for Prandtl numbers of: 0.5, 0.7, 1.0, 1.6, 3.2 and 10.

Solutions for Prandtl numbers less than 0.5 are excluded by the grid size. This may be seen from inspection of the coefficient of the second temperature term in (11), which indicates the interdependence of $PR, \Delta X,$

and ΔY . In order to obtain convergence, PR must be large enough to prevent this term from becoming negative. Thus low Prandtl numbers, approaching those of liquid metals, cannot be effectively handled by finite-difference methods owing to the large number of calculations required by the small grid.

The computer program, written in Fortran 60, is included in the Appendix.

III. RESULTS

Tables I through VI contain computed and extrapolated values of the heat transfer rates as a function of distance from the entrance for each of the thermal boundary conditions for a Prandtl number of 0.7. Figures 5 through 29 contain curves of the transfer rate versus downstream position and temperature and velocity profiles for Prandtl numbers of 0.5, 0.7, 1.0, 1.6, 3.2 and 10.

With the exception of the Asymmetric Constant Wall Temperature Case, which is expressed in terms of the dimensionless heat flux parameter, q^* ; the heat transfer rates are presented as local Nusselt number variation with the length parameter, L . Whereas, the computations were carried out using the dimensionless length parameter X , which is normally employed for hydrodynamic developments; L , based on the hydraulic diameter is customarily employed in heat transfer. The conversion is:

$$X = 16L$$

The use of all finite starting length" in the finite difference equations results in a finite initial value for the Nusselt number at $X = 0$ rather than the theoretically infinite value at the entrance. This causes a nearly flat slope near the entrance and an artificial inflection point in the Nusselt number versus length curve. The inflection point occurs progressively farther downstream with the increasing Prandtl number, thereby limiting the

the useful span of the curves. A reduction of grid size from $\Delta X = .001$, $\Delta Y = .1$ to $\Delta X = .0001$, $\Delta Y = .05$ was observed to double the initial Nusselt number from 40 to 80, and move the inflection point upstream. This increased the useful span. However, the approach obviously reaches a practical limit very rapidly due to the number of calculations and the accuracy required of the hydrodynamic solution very close to the entrance.

In general, for the three thermal boundary conditions in which the Nusselt number was used as a heat transfer parameter, the curves for Prandtl numbers of 0.5, 0.7, 1.0 and 1.6 behave as expected for values of $L > 10^{-4}$. For Prandtl numbers of 3.2 and 10, $L = 10^{-3}$ is the approximate lower limit of validity.

Constant Heat Input. A comparison of local Nusselt numbers obtained in the present analysis with those reported by Siegel and Sparrow \overline{Nu}_7 , and Han \overline{Nu}_6 , contained in Fig. 5, indicate close agreement with the results of Siegel and Sparrow. Their solution employed a simplified energy equation in which the temperature distribution in the boundary layer was expressed as a series of polynomials in the transverse coordinate using the downstream station as a parameter. The hydrodynamic solution employed Schiller's approximation.

The comparison with Han's integro-numerical solution is not as close as might appear in Fig. 5 since this curve is for a Prandtl number of 0.8

and should lie above the other two curves which are for a Prandtl number of 0.7.

The computed curves of local Nusselt number versus length contained in Fig. 6. for Prandtl numbers of 0.5, 0.7, 1.0, 1.6, 3.2, and 10, may be approximated within 10 per cent, for $0.5 \leq PR \leq 1.6$, and $L > 10^{-3}$ by the following;

$$Nu_x = 8.24 + \frac{.0186 (PR/L)}{1 + .0178 (PR/L)^{.6}}$$

Velocity and temperature profiles for constant heat input are contained in Figs. 7 through 10.

Constant Wall Temperature (Symmetric Case). Local values of Nusselt numbers for this boundary condition are compared in Fig. 11 with those of Sparrow $\overline{[5]}$, which were computed using the Karman-Pohlhausen method and Schiller's hydrodynamic solution. Again close correlation is indicated between the two results.

The local Nusselt number curves of Fig. 12 may be approximately represented within 10 per cent for $0.5 \leq PR \leq 1.6$, and $L > 10^{-3}$ by the following;

$$Nu_x = 7.60 + \frac{.0148 (PR/L)}{1 + .0143 (PR/L)^{.6}}$$

Velocity and temperature profiles for this boundary condition are contained in Figs. 13 through 16.

One Wall Constant Temperature - One Wall Insulated. The results of this computation are presented in Fig. 17. The local Nusselt number may be approximated within 10 per cent for $0.5 \leq PR \leq 1.6$, and $L > 10^{-3}$ by;

$$N_{u_x} = 4.84 + \frac{.0155 (PR/L)}{1 + .012 (PR/L)^{.6}}$$

The velocity and temperature distributions are illustrated in Figs. 18 through 21.

Constant Wall Temperature (Asymmetric Case). Dimensionless heat flux values for this boundary condition are presented in Figs. 22, 23 and 24 for $\frac{N_1 - 1}{N_2 - 1}$ ratios of 1/2, 1/3, and 1/4.

Note that the upper (hotter) wall curve is smoothly asymptotic to the value predicted for the steady state condition. The lower curve exhibits a much shallower initial slope, passes through an inflection point, and then, approaches a negative asymptotic value of the same magnitude and at the same rate as the upper wave.

Velocity and temperature profiles for $\frac{N_1 - 1}{N_2 - 1} = 1/4$ are presented in Figs. 25 through 28.

The behavior of the local Nusselt number for this asymmetrical case is depicted in Fig. 29. The lower curve, representing the local Nusselt number variation for the lower (cooler) wall, does not depict the actual physical situation.

Both the denominator and the numerator of;

$$N_{u_x} = \frac{4 (T_w - T_{w-\Delta Y})}{\Delta Y} \frac{1}{T_w - T_m} \quad (18)$$

approach zero at different rates. The curve tends to positive infinity as the denominator approaches zero, returns from negative infinity, and becomes zero as the numerator goes to zero; and finally approaches the actual steady asymptotic value.

IV. CONCLUSIONS

From the results of this study it may be concluded that:

1. The finite difference method, as employed in this analysis, yields results which are consistent with previous solutions for other geometries $\sqrt{2}$ and which are asymptotic to the known fully developed values. The method is, however, limited to a small range of Prandtl numbers near unity by the small grid sizes necessary outside this range. For small Prandtl numbers the grid must be very small to obtain convergence, while for large Prandtl numbers practical grid dimensions result in significant inaccuracies near the entrance due to the "finite starting length".
2. The results of the approximate integral methods suggested by Siegel and Sparrow $\sqrt{7}$ for constant heat input, and by Sparrow $\sqrt{5}$ for constant wall temperature, compare very favorably with the finite difference solutions reported here. This additional substantiation of the methods suggested by these authors is significant because of the practical utility of their approach, which requires relatively few calculations, is capable of handling a wide range of Prandtl numbers, and can predict heat transfer rates very close to the entrance.

REFERENCES

1. Miller, James A.: Heat Transfer at the Entrance to a Region Surrounded by Parallel Flat Plates, Illinois Institute of Technology, Unpublished.
2. Kays, W. M.: Numerical Solutions for Laminar Flow Heat Transfer in Circular Tubes, 1953, Technical Report No. 20, Stanford Univ.
3. Bodoia, John R.: The Finite Difference Analysis of Confined Viscous Flows, 1959, Phd. Thesis, Carnegie Institute of Technology, Pittsburgh.
4. Schlichting, H.: Boundary Layer Theory, 1955, McGraw-Hill Book Co., Inc., New York.
5. Sparrow, E. M.: Analysis of Laminar Forced-Convection Heat Transfer in Entrance Region of Flat Rectangular Ducts, NACA, TN3331, 1954.
6. Hans, L. S.: Simultaneous Developments of Temperature and Velocity Profiles in Flat Ducts, International Developments in Heat Transfer, Proceedings of the 1961 International Heat Transfer Conference at Boulder, Colorado, Part III.
7. Siegel, Robert and E. M. Sparrow: Simultaneous Development of Velocity and Temperature Distributions in a Flat Duct with Uniform Wall Heating, A. I. Ch. E. Journal, V. S., March 1959: 73-75.

TABLE I
CONSTANT HEAT INPUT
PR = 0.7

X	L	N_{u_x}	T_w
.0016	.0001	46.2	1.09
.0032	.0002	30.0	1.14
.0064	.0004	23.7	1.18
.0128	.0008	18.0	1.24
.0160	.0010	16.6	1.26
.0320	.0020	12.9	1.35
.0640	.0040	10.3	1.47
.1280	.0080	8.87	1.62
.1600	.0100	8.62	1.67
	Asymptotic to	8.24	

TABLE II
CONSTANT WALL TEMPERATURE
(SYMMETRIC CASE)

PR = 0.7

X	L	N_{u_x}
.0016	.0001	34.0
.0032	.0002	26.0
.0064	.0004	19.9
.0128	.0008	15.3
.0160	.0010	13.7
.0320	.0020	10.5
.0640	.0040	8.58
.1280	.0080	7.78
.1600	.0010	7.63
	Asymptotic to	7.60

TABLE III

ONE WALL CONSTANT TEMPERATURE - ONE WALL INSULATED

PR = 0.7

X	L	N_{u_x}	T_w
.0016	.0001	33.0	1.000
.0032	.0002	24.0	1.000
.0064	.0004	19.2	1.000
.0128	.0008	13.0	1.000
.0160	.0010	11.6	1.000
.0320	.0020	9.05	1.000
.0640	.0040	7.20	1.000
.1280	.0080	5.93	1.001
.1600	.0100	5.55	1.021
.4000	.0250	4.96	1.139
	Asymptotic to	4.84	2.000

TABLE IV
 CONSTANT WALL TEMPERATURE
 (ASYMMETRIC CASE)

$$\frac{N_1 - 1}{N_2 - 1} = 1/2 \quad PR = 0.7$$

X	L	q_1^*	q_2^*
.0032	.0002	26.2	57.5
.0064	.0004	17.3	41.4
.0128	.0008	11.9	28.7
.0160	.0010	10.7	25.9
.0320	.0020	8.08	18.7
.0460	.0040	6.18	13.7
.1280	.0080	4.73	10.1
.1600	.0100	4.24	9.15
.3200	.0200	2.24	6.35
.6400	.0400	-.19	3.81
.9600	.0600	-1.23	2.76
	Asymptotic to	-2.00	+2.00

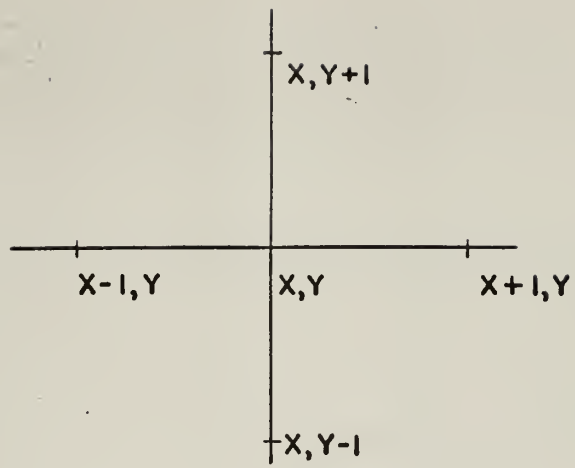
TABLE V
 CONSTANT WALL TEMPERATURE
 (ASYMMETRIC CASE)

$$\frac{N_1 - 1}{N_2 - 1} = 1/3 \quad PR = 0.7$$

X	L	q_1^*	q_2^*
.0032	.0002	28.0	86.0
.0064	.0004	17.3	62.0
.0128	.0008	11.8	43.0
.0160	.0010	10.8	38.9
.0320	.0020	8.09	28.1
.0640	.0040	6.18	20.6
.1280	.0080	4.69	15.2
.1600	.0100	4.15	13.8
.3200	.0200	1.65	9.84
.6400	.0400	-1.58	6.41
.9600	.0600	-2.97	5.02
	Asymptotic to	-4.00	+4.00

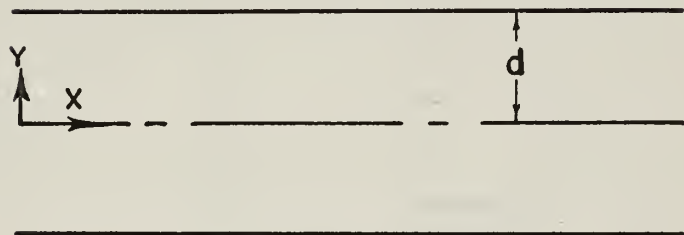
TABLE VI
 CONSTANT WALL TEMPERATURE
 (ASYMMETRIC CASE)

X	$\frac{N_1 - 1}{N_2 - 1} = 1/4$	PR = 0.7	q_1^*	q_2^*
	L			
.0032	.0002		28.2	116.0
.0064	.0004		16.8	82.9
.0128	.0008		12.2	57.7
.0160	.0010		10.5	50.4
.0320	.0020		8.09	37.5
.0640	.0040		6.17	27.5
.1280	.0080		4.66	20.3
.1600	.0100		4.06	18.4
.3200	.0200		1.06	13.3
.6400	.0400		-2.96	9.03
.9600	.0600		-4.71	7.27
	Asymptotic to		-6.00	+6.00



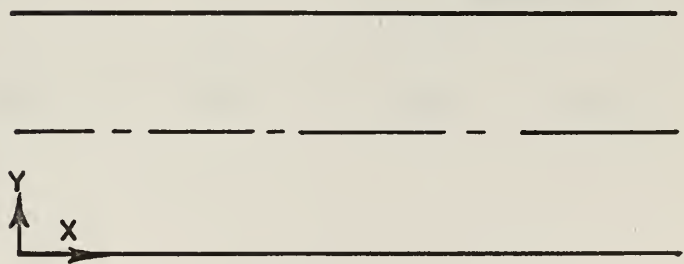
(a)

DESIGNATION OF MESH POINTS



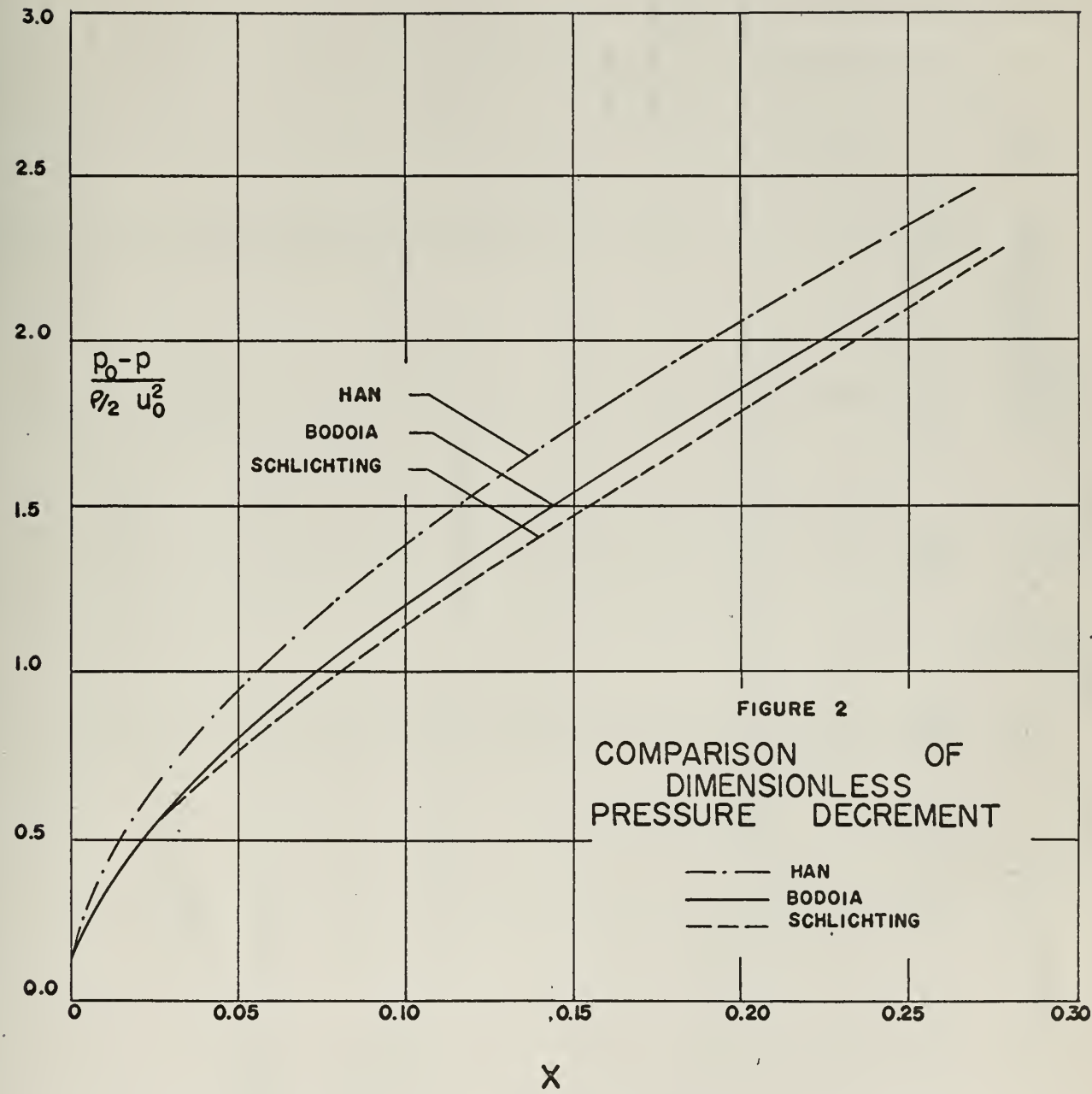
(b)

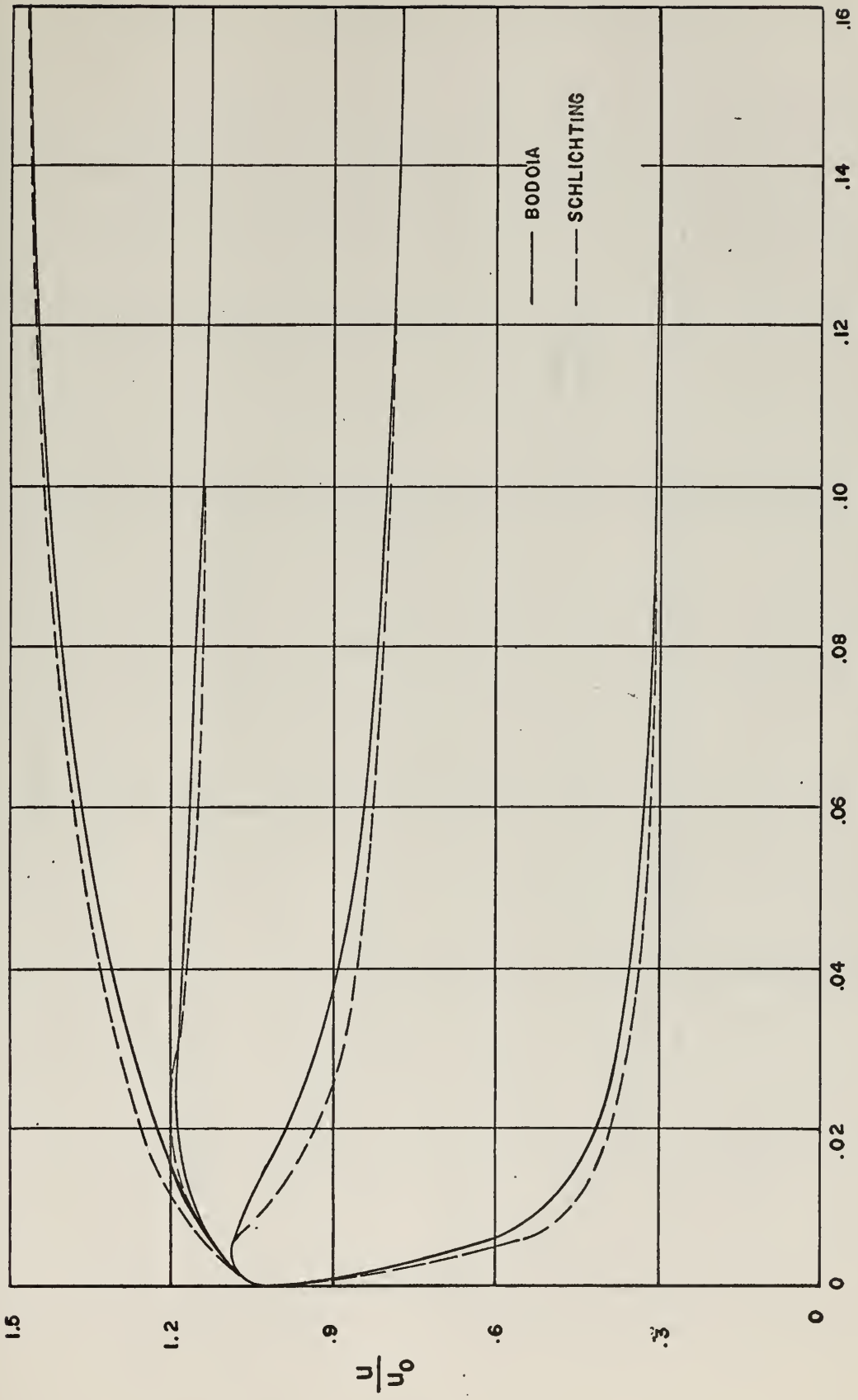
AXIS SYSTEM, SYMMETRICAL CASES;
CONSTANT WALL TEMPERATURE
CONSTANT HEAT INPUT



(c)

AXIS SYSTEM, NON-SYMMETRICAL CASES;
ONE WALL INSULATED;
CONSTANT, BUT DIFFERENT WALL TEMPERATURES

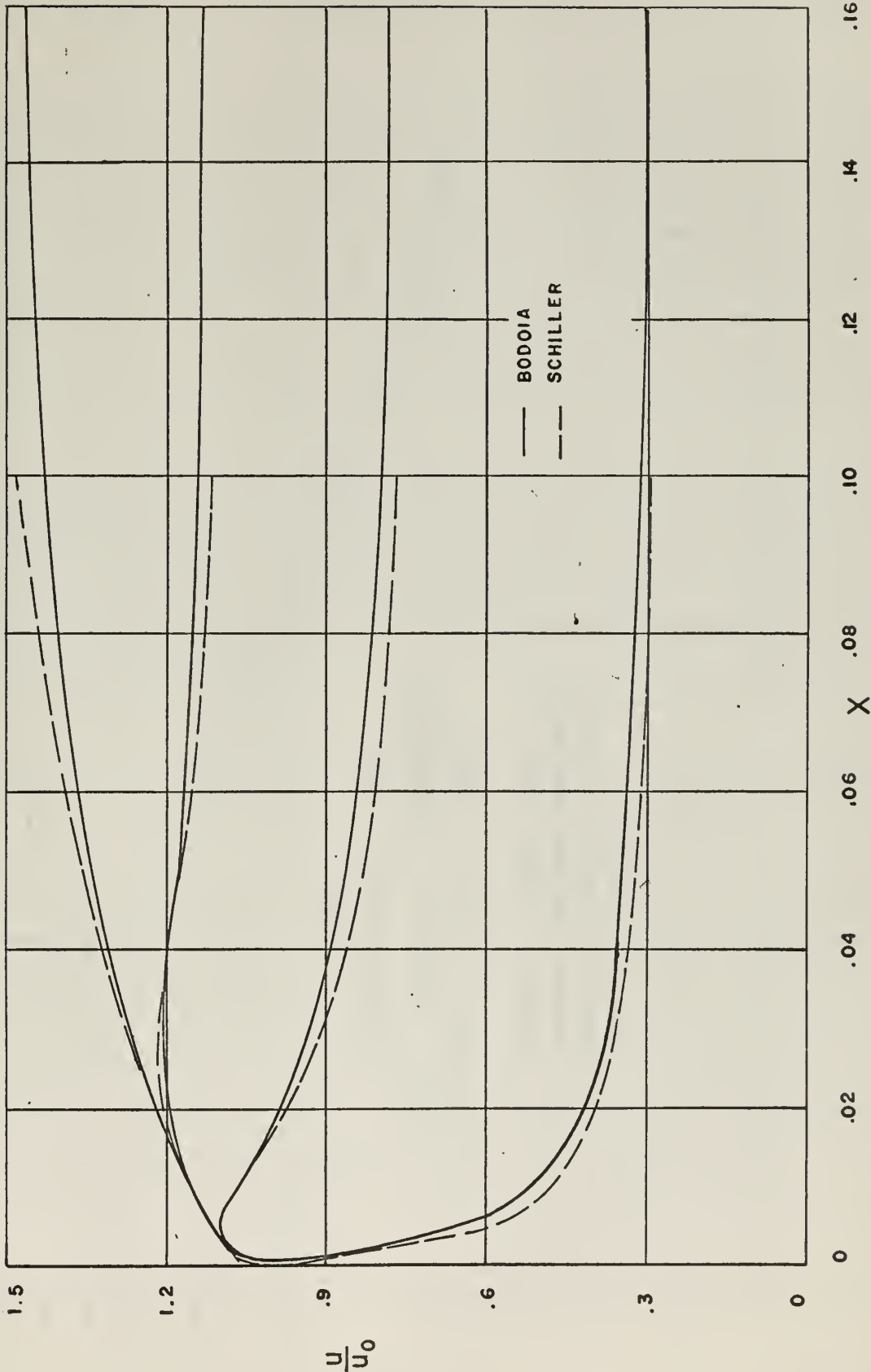




COMPARISON OF VELOCITY DISTRIBUTIONS OF
BODOIA AND SCHLICHTING

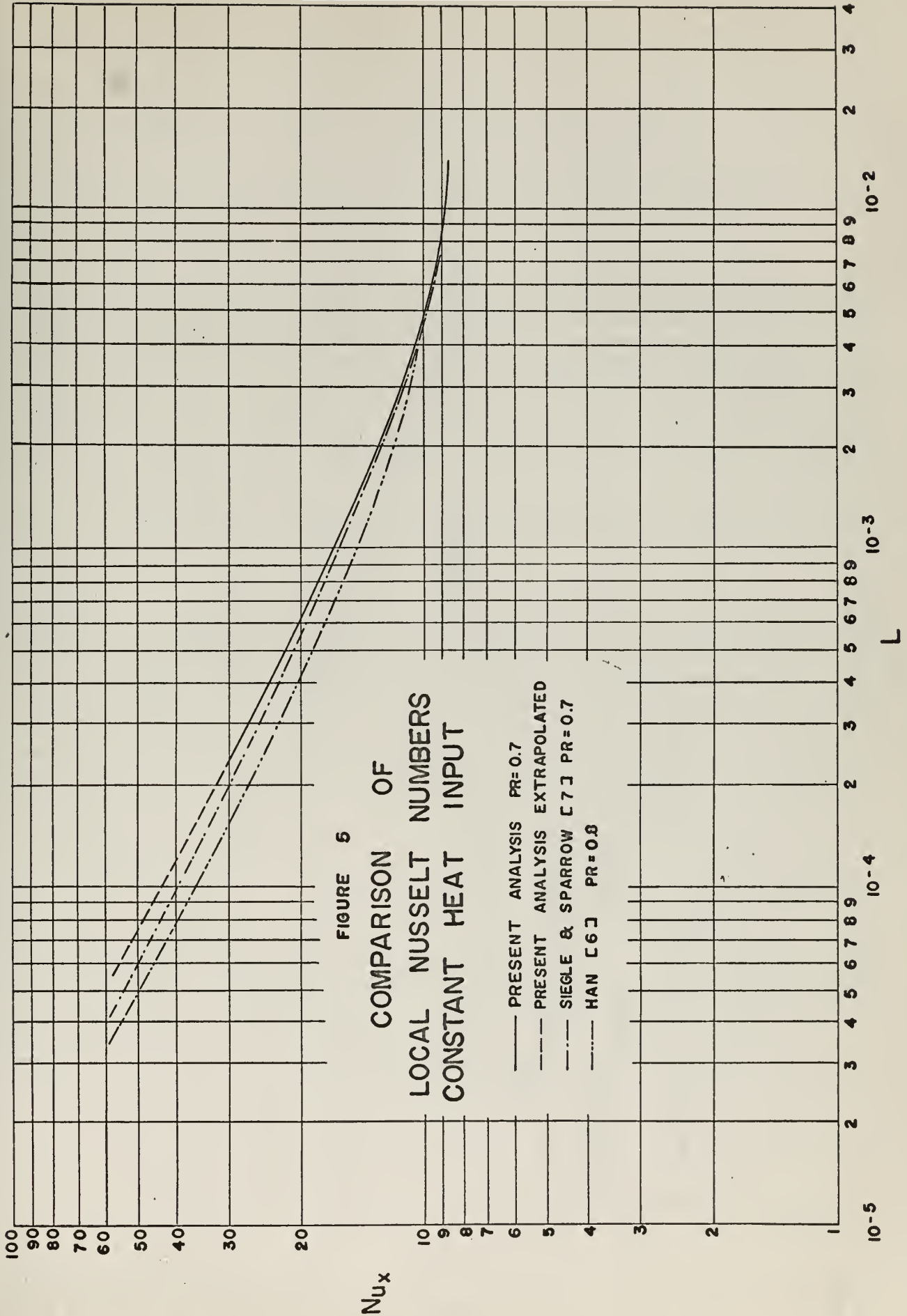
FIGURE 3





COMPARISON OF VELOCITY DISTRIBUTIONS DUE TO
BODOIA AND SCHILLER

FIGURE 4



Nu_x

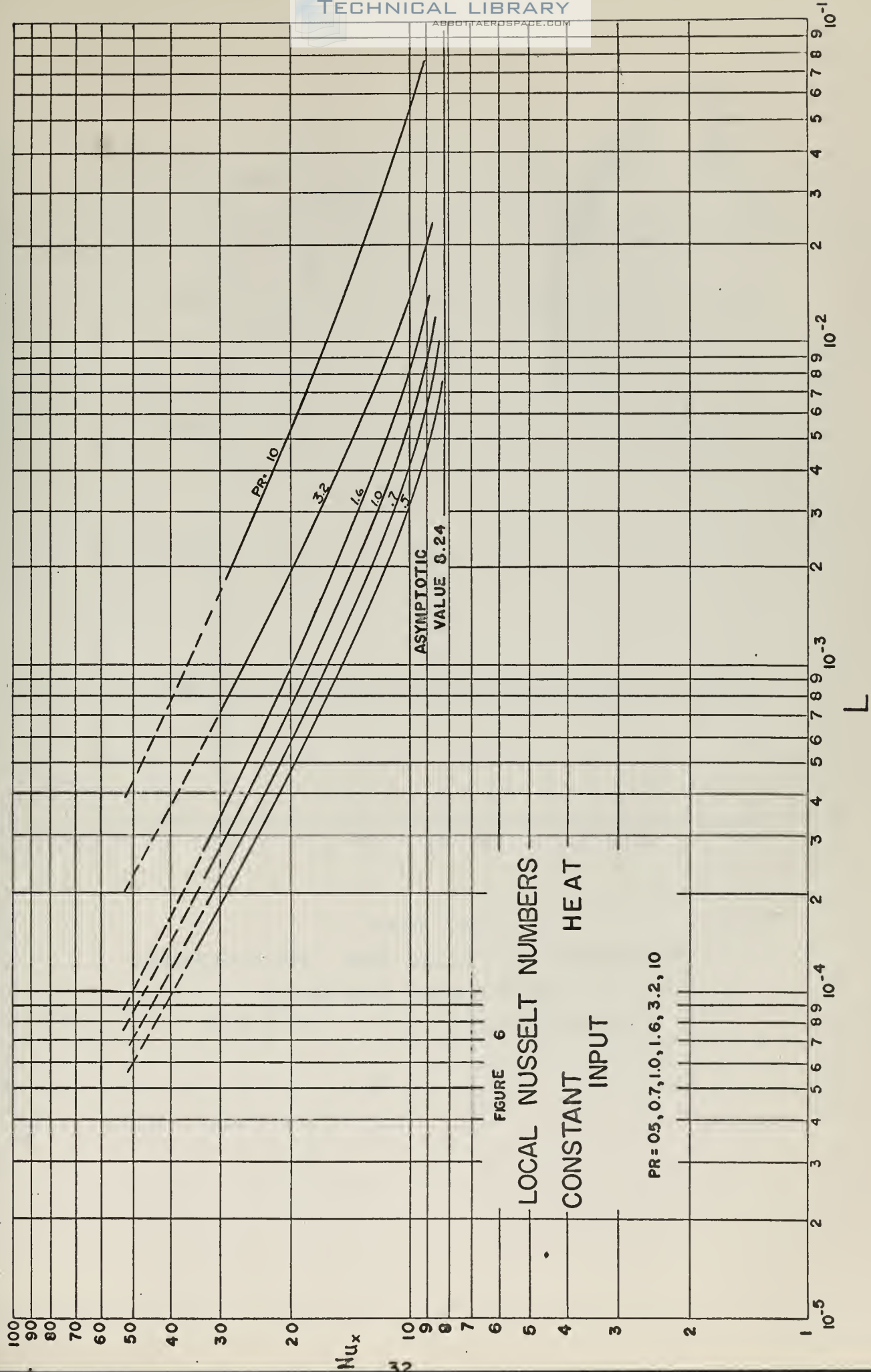


FIGURE 6
 LOCAL NUSSLETT NUMBERS
 CONSTANT INPUT HEAT

$Pr = 0.5, 0.7, 1.0, 1.6, 3.2, 10$

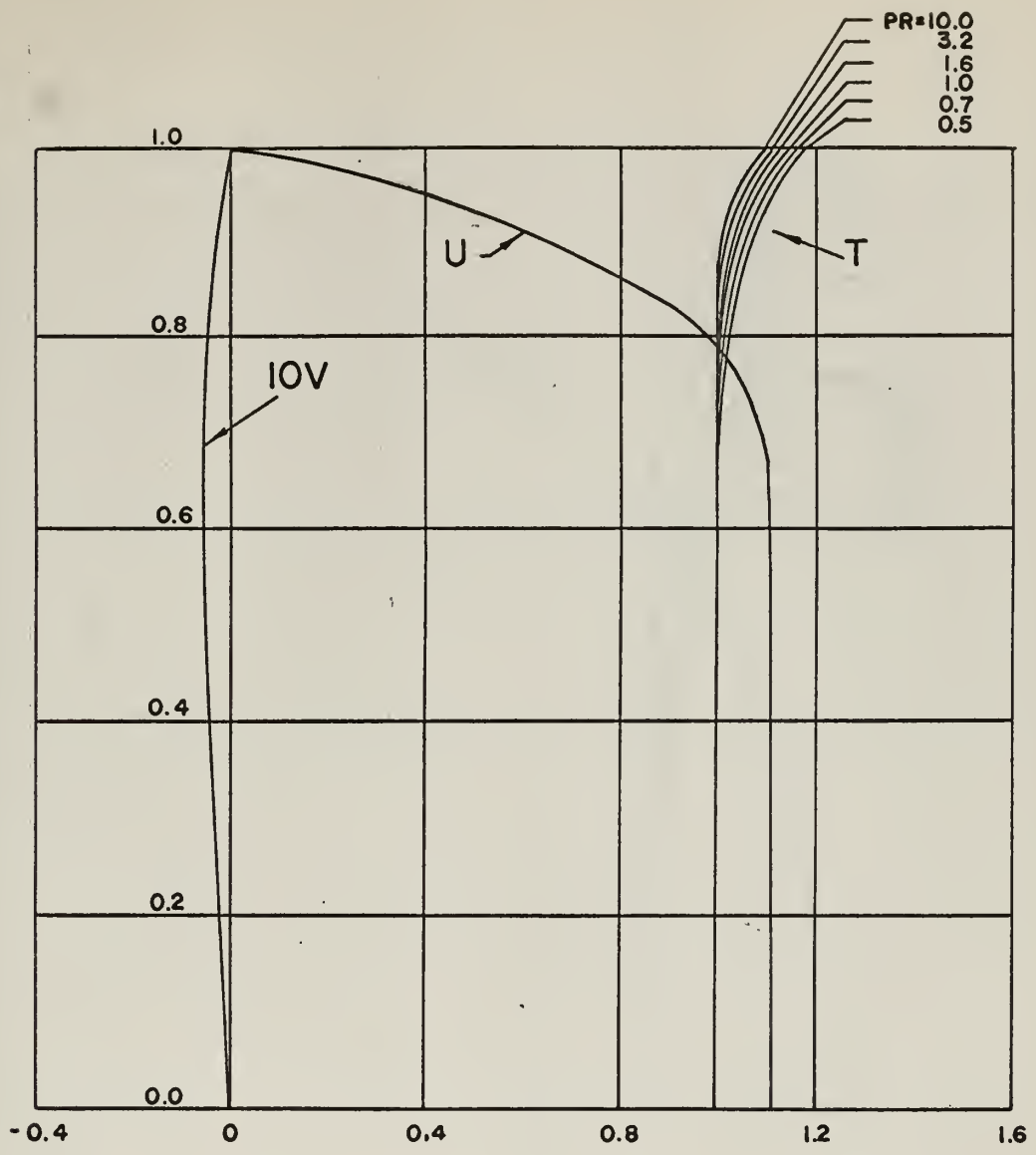


FIGURE 7
TEMPERATURE AND VELOCITY PROFILES
CONSTANT HEAT INPUT
 $X=0.005$ $L=0.0003125$



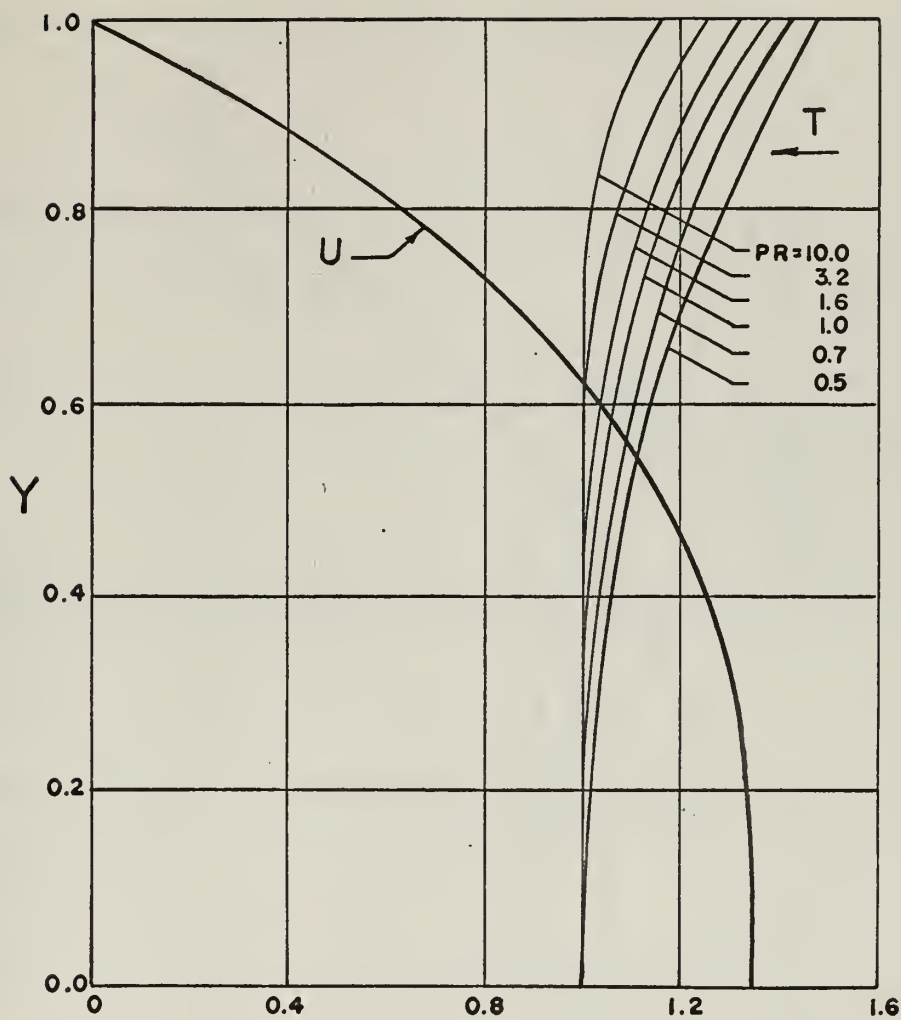


FIGURE 8

TEMPERATURE AND VELOCITY PROFILES
X=0.050 L=0.003125



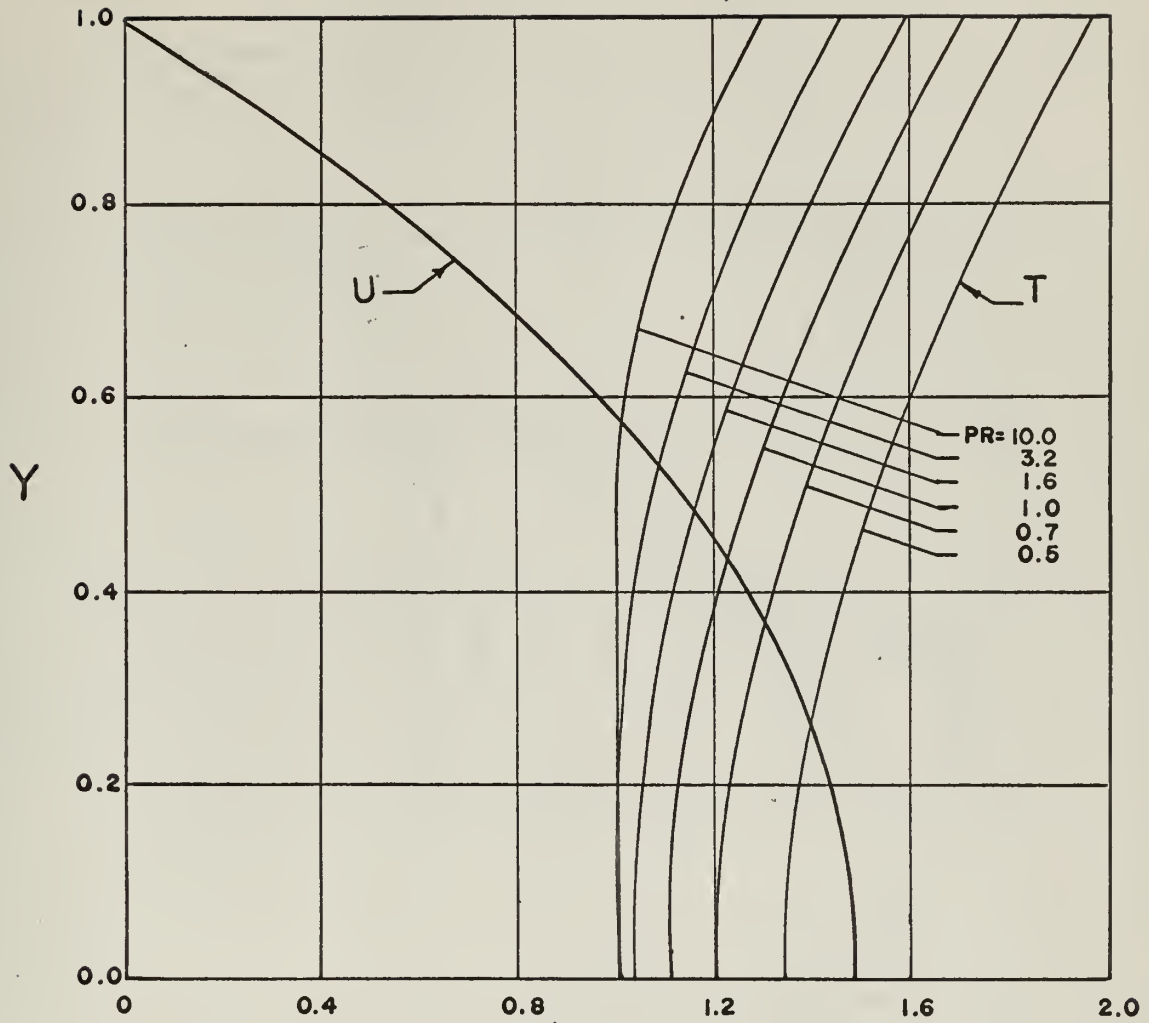


FIGURE 9

TEMPERATURE AND VELOCITY PROFILES

$X = 0.250$

$L = 0.0156$

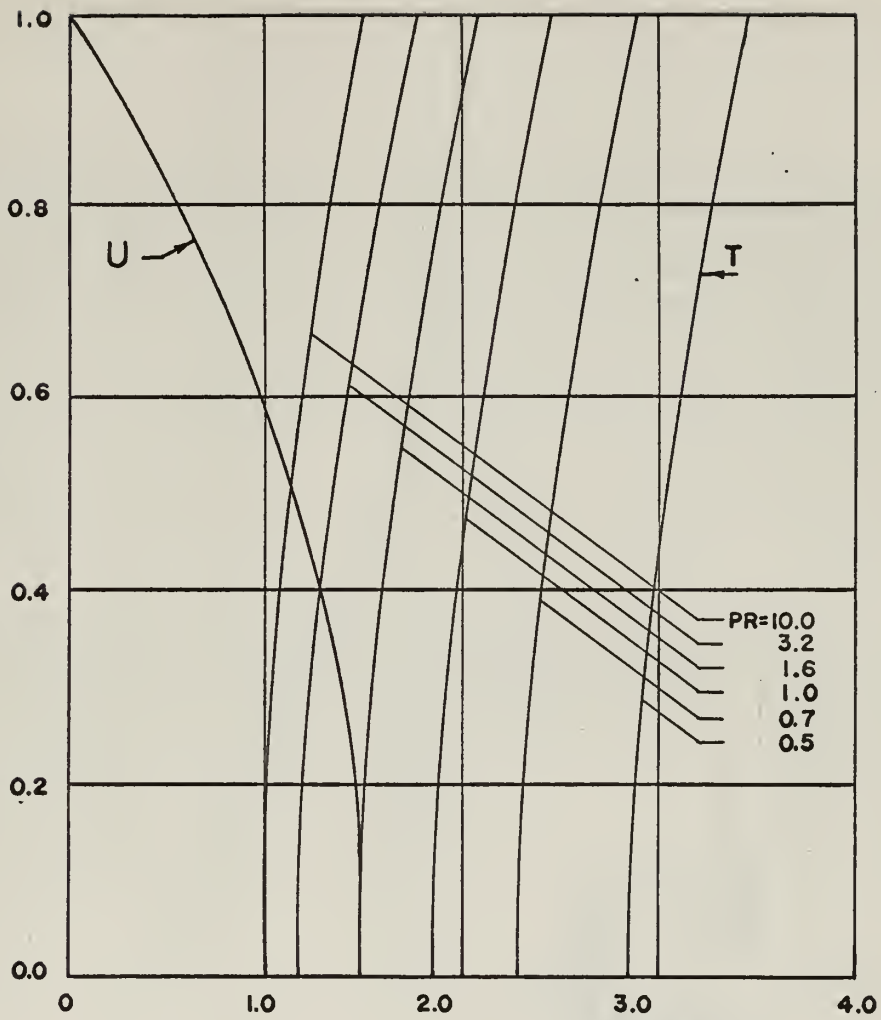


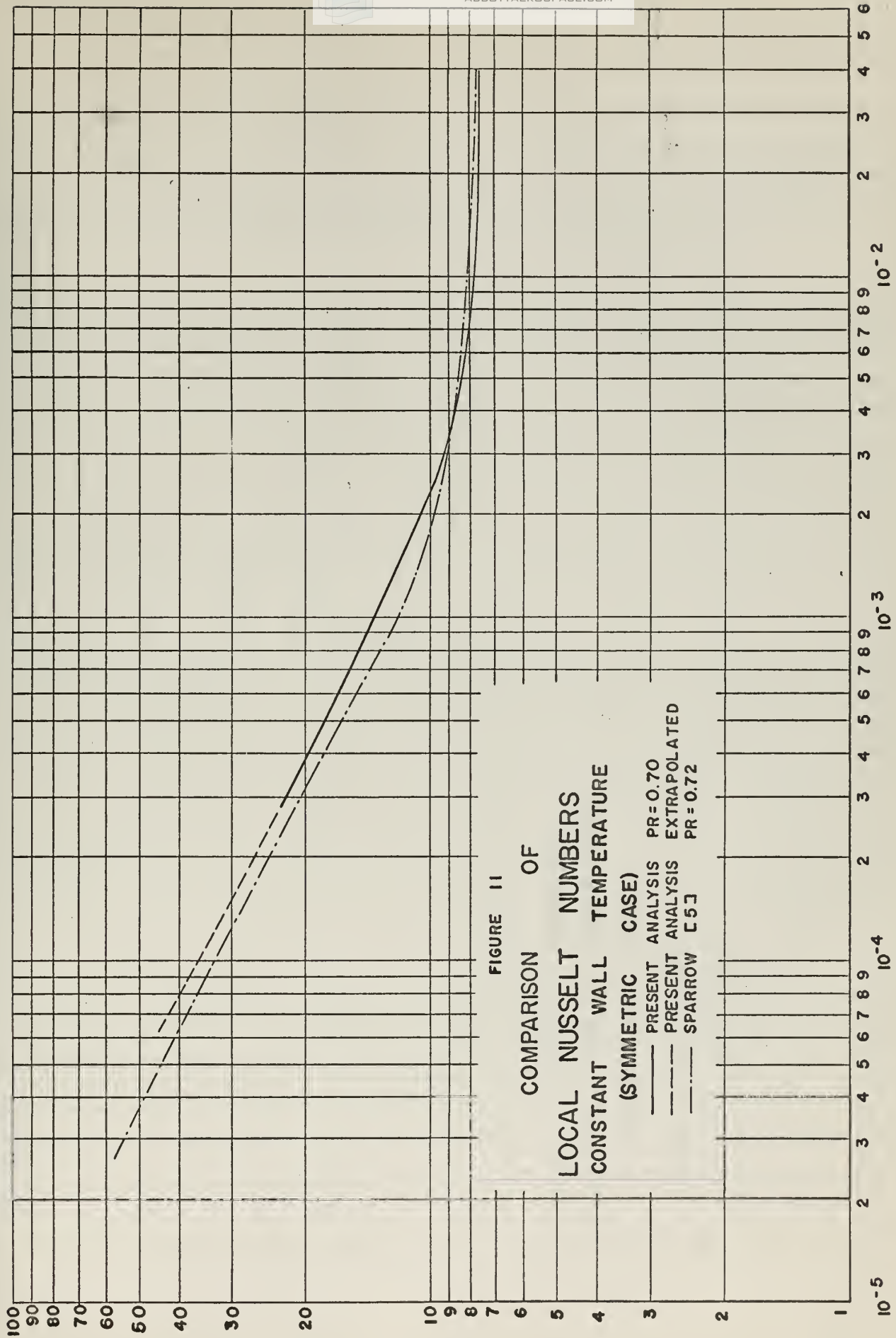
FIGURE 10

TEMPERATURE AND VELOCITY PROFILES

X = 1.00

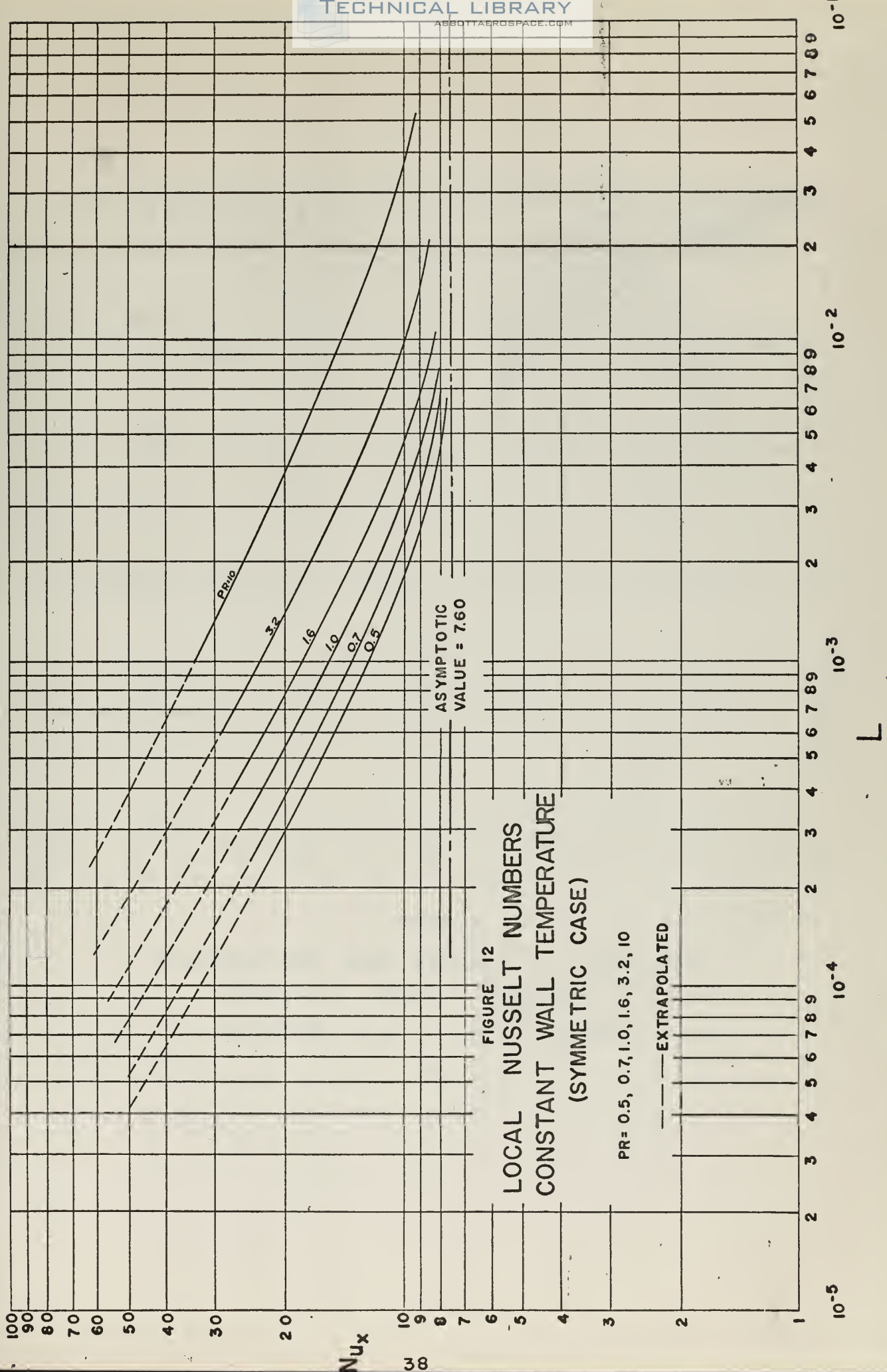
L = 0.0625





Nu_x

L



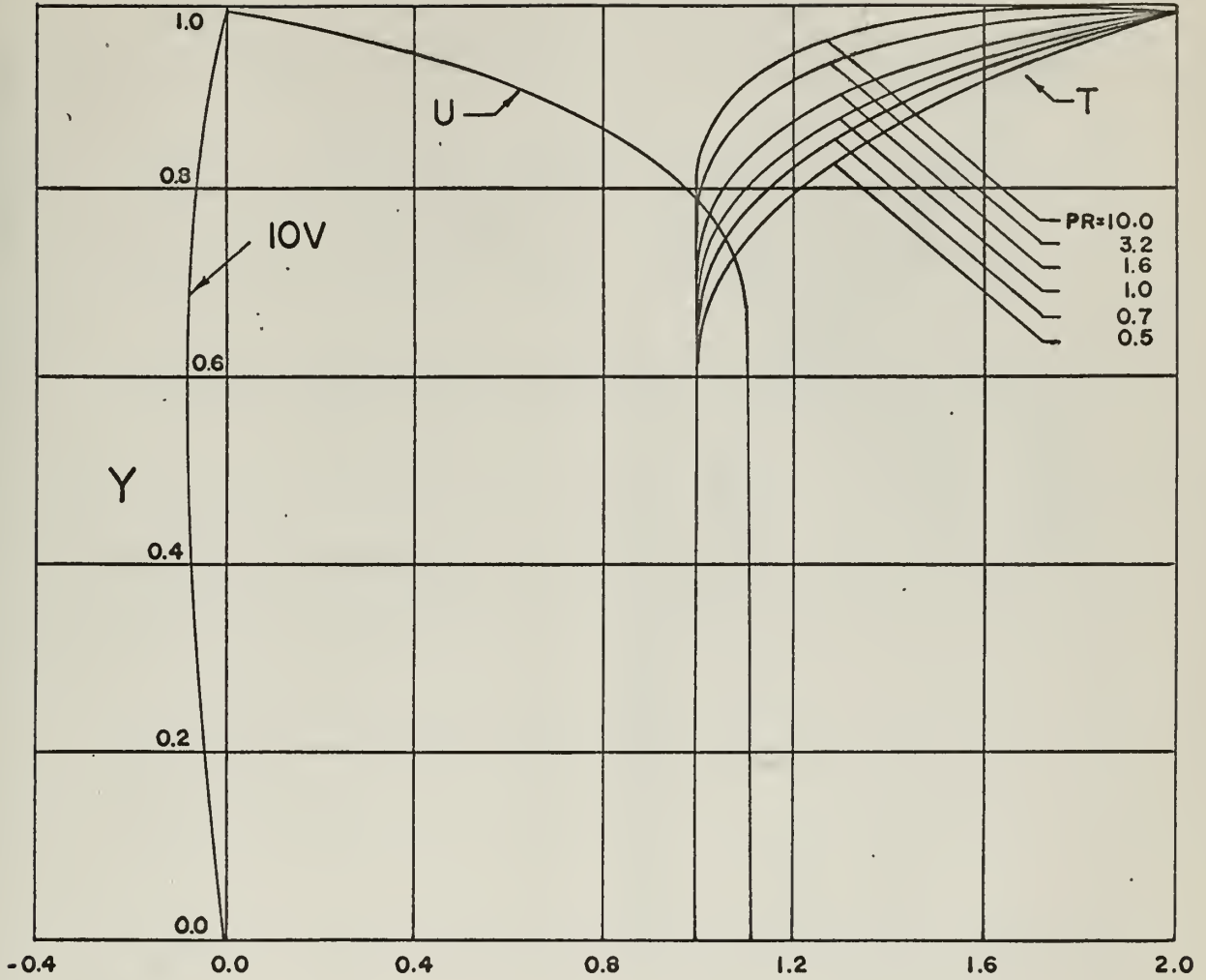


FIGURE 13
TEMPERATURE AND VELOCITY PROFILES
CONSTANT WALL TEMPERATURE
X=0.005 L = 0.0003125

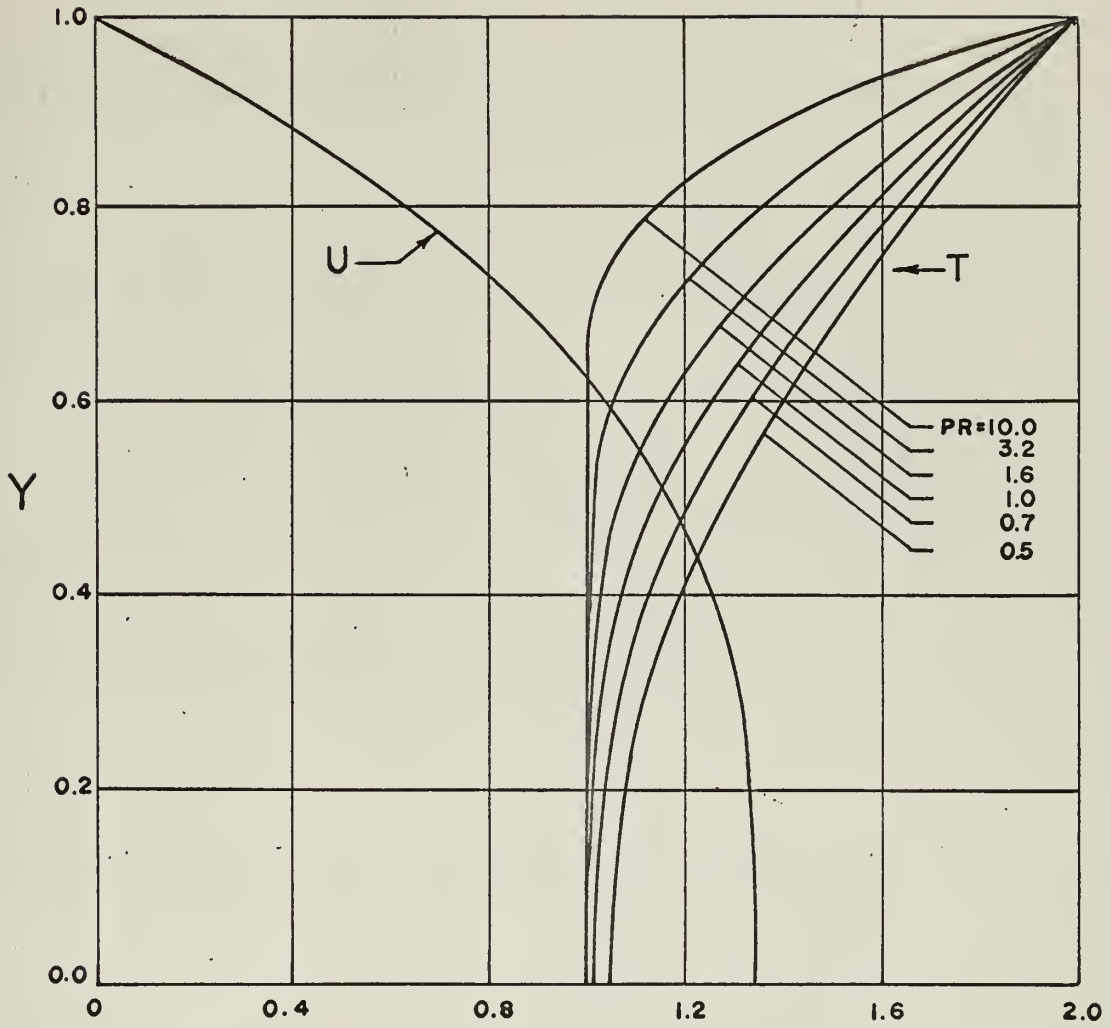


FIGURE 14

TEMPERATURE AND VELOCITY PROFILES
CONSTANT WALL TEMPERATURE
 $X = 0.050$ $L = 0.003125$

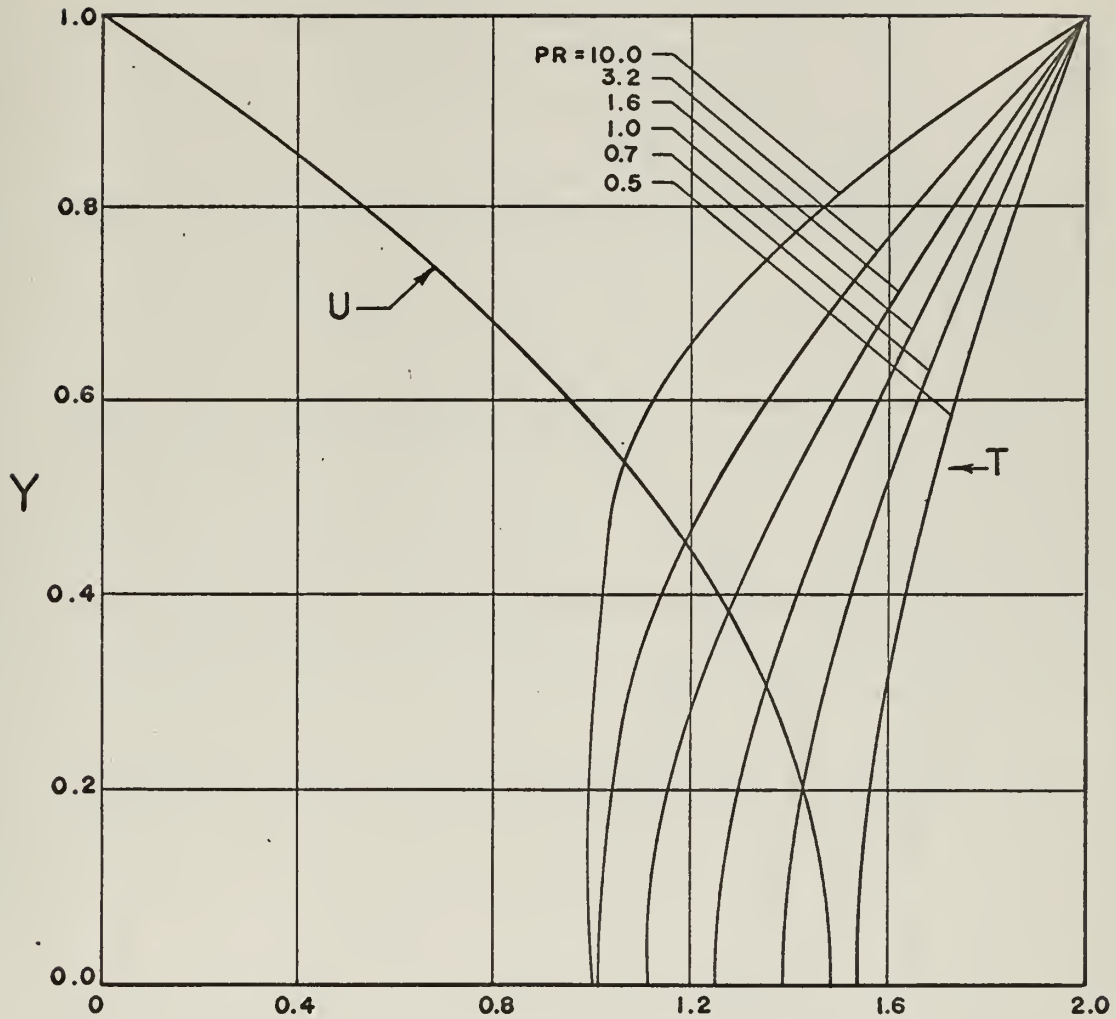


FIGURE 15
TEMPERATURE AND VELOCITY PROFILES
CONSTANT WALL TEMPERATURE
X = 0.250 L = 0.0156

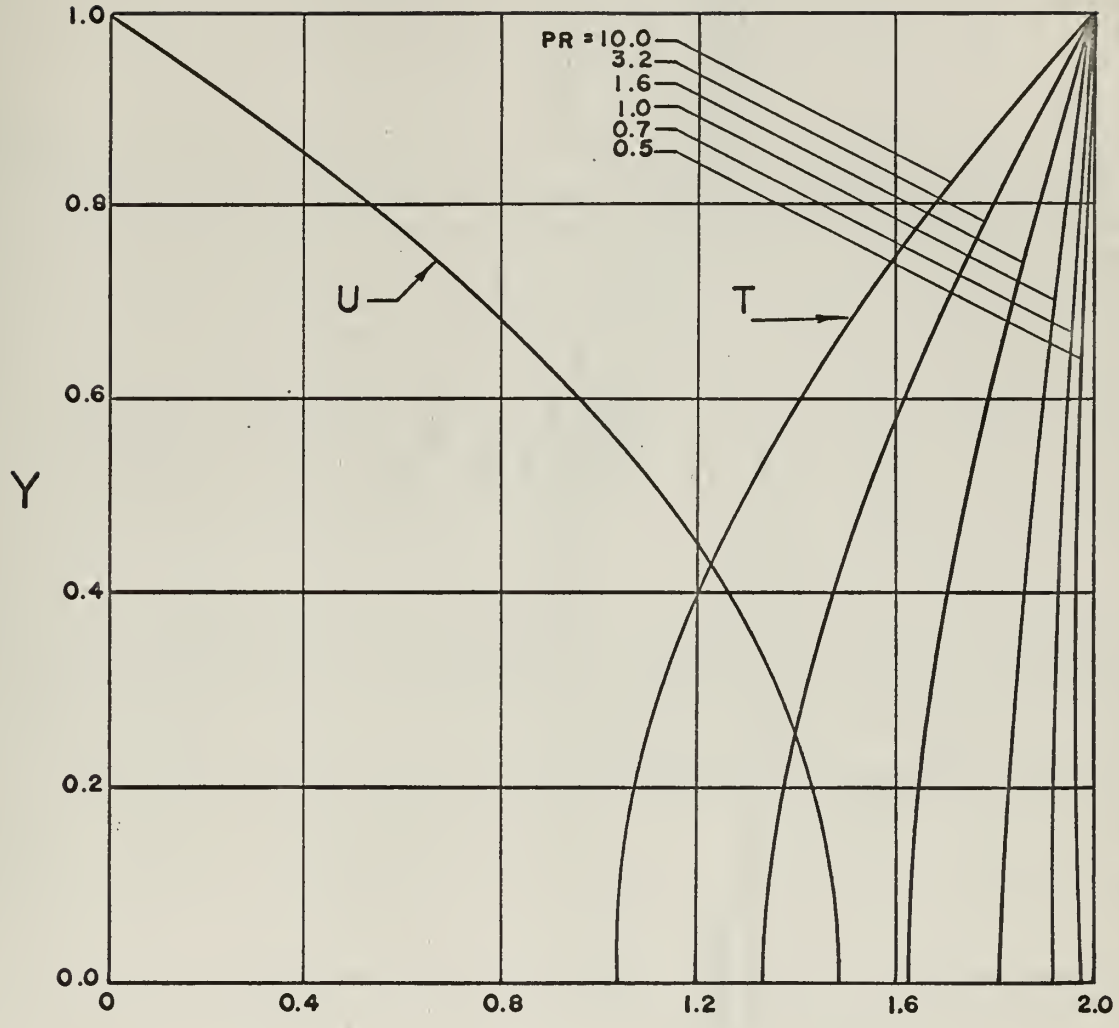


FIGURE 16

TEMPERATURE AND VELOCITY PROFILES
CONSTANT WALL TEMPERATURE
X = 1.00 L = 0.0625



Very faint text, likely a title or description of the drawing, which is illegible due to the image quality.

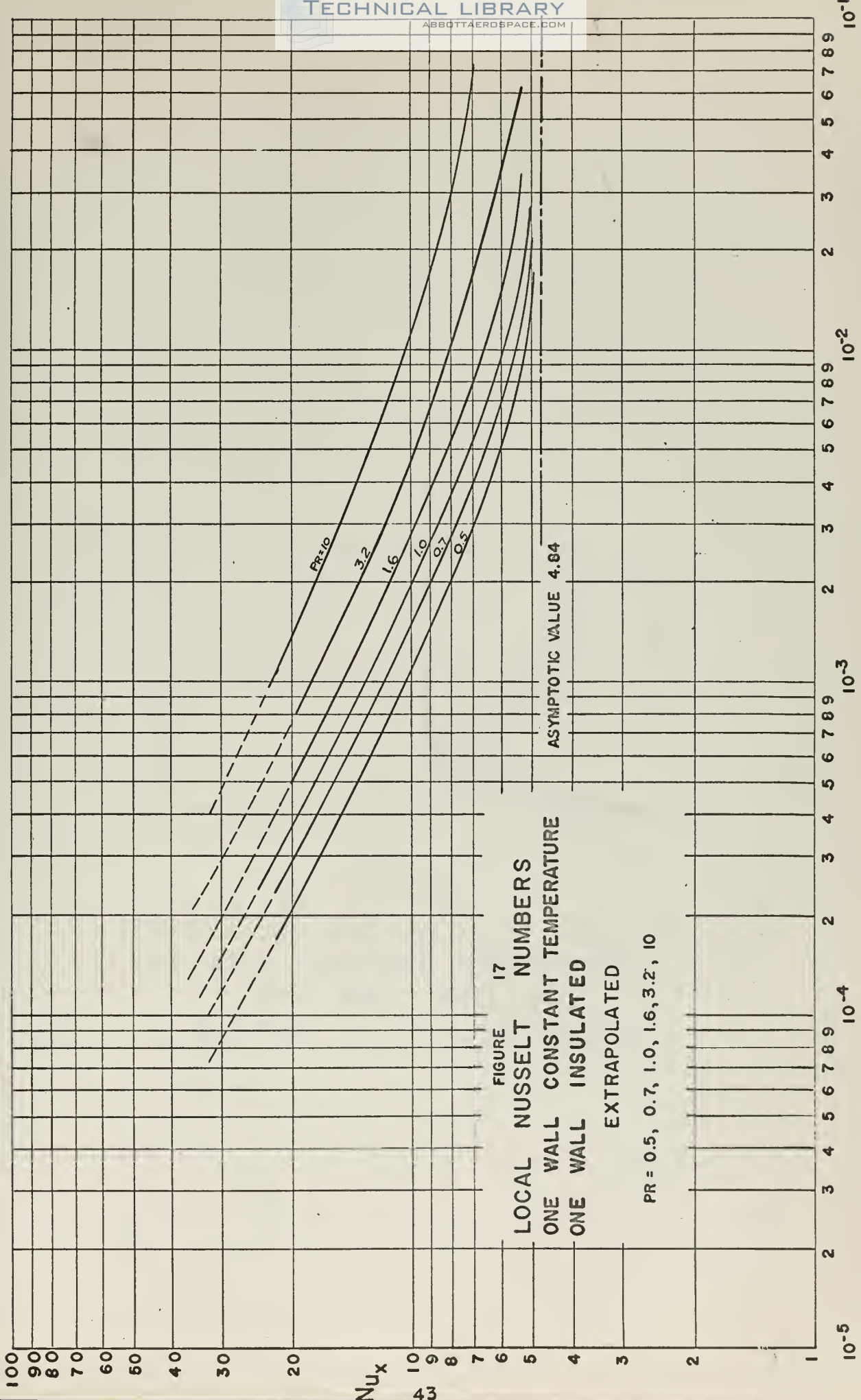


FIGURE 17
LOCAL NUSSOLT NUMBERS
ONE WALL CONSTANT TEMPERATURE
ONE WALL INSULATED
 EXTRAPOLATED

PR = 0.5, 0.7, 1.0, 1.6, 3.2, 10

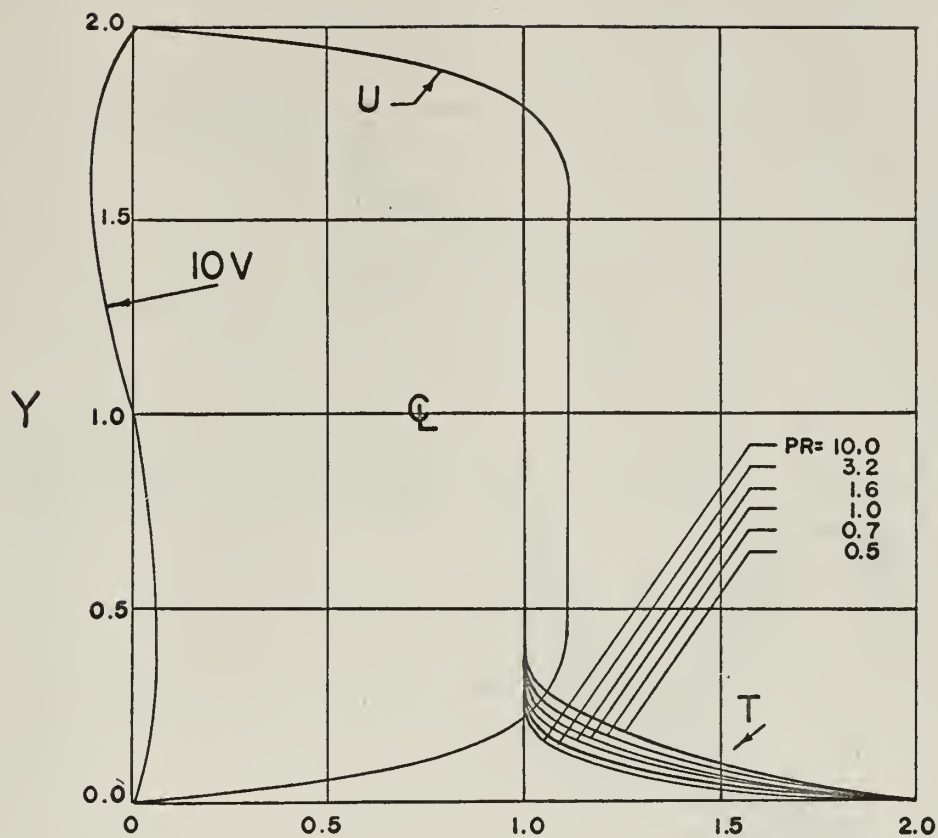


FIGURE 18

TEMPERATURE AND VELOCITY PROFILES
ONE WALL CONSTANT TEMPERATURE
ONE WALL INSULATED
X= 0.005 L = 0.0003125

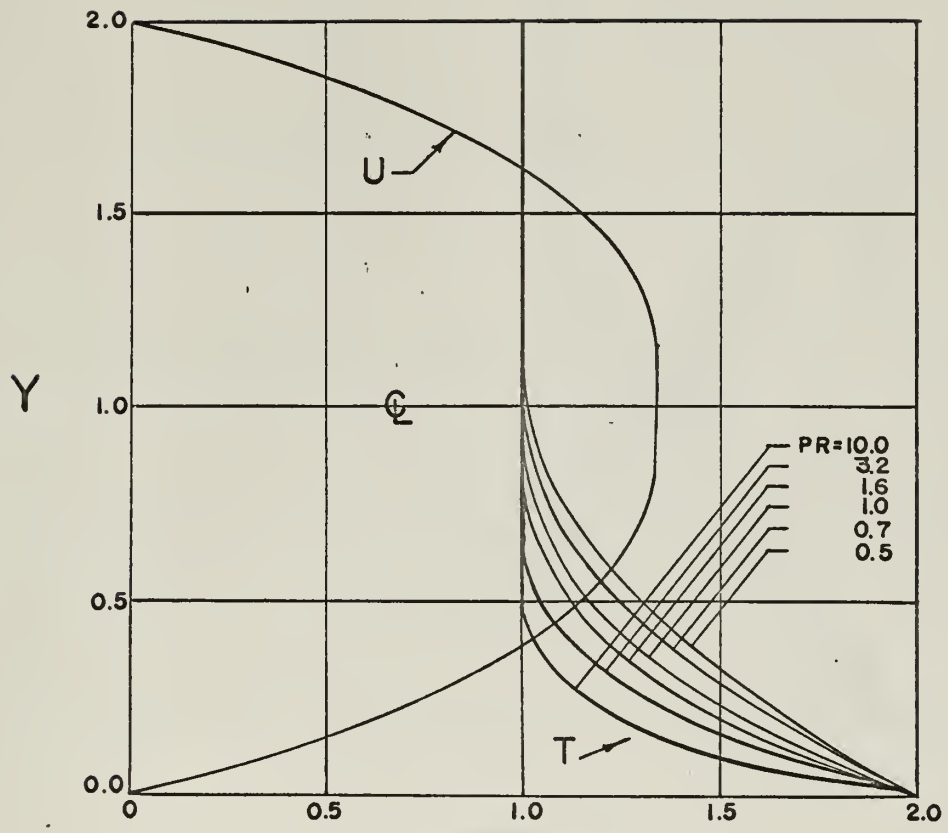


FIGURE 19
TEMPERATURE AND VELOCITY PROFILES
ONE WALL CONSTANT TEMPERATURE
ONE WALL INSULATED
X=0.050 L = 0.003125

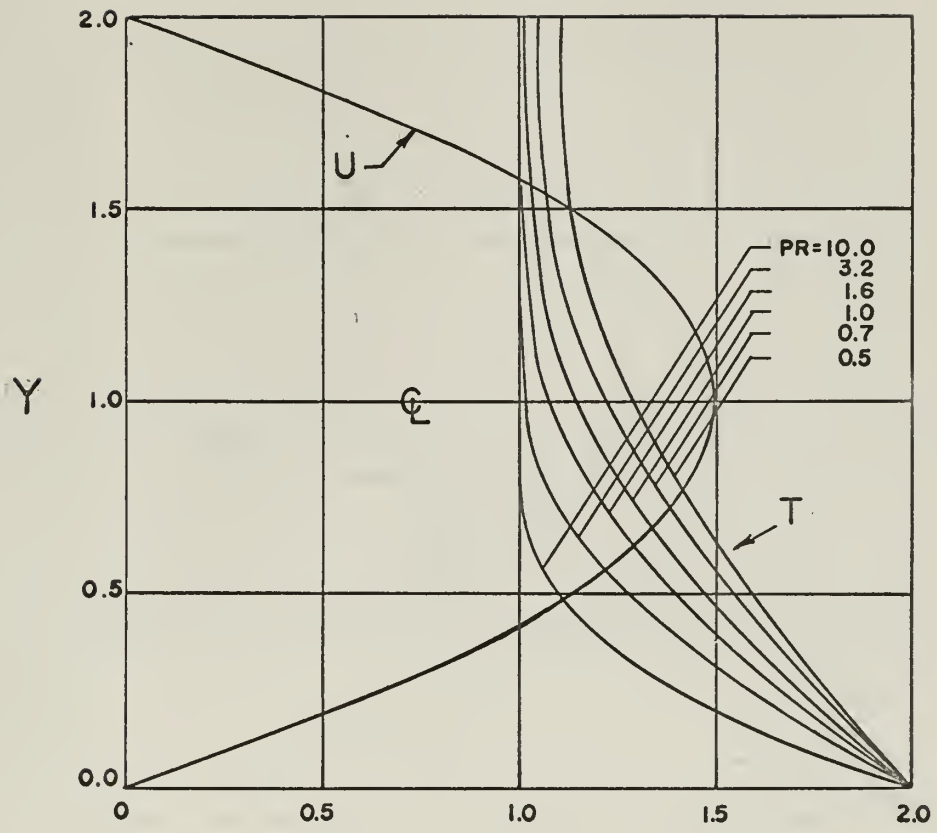


FIGURE 20

TEMPERATURE AND VELOCITY PROFILES
ONE WALL CONSTANT TEMPERATURE
ONE WALL INSULATED
X=0.250 L = 0.0156

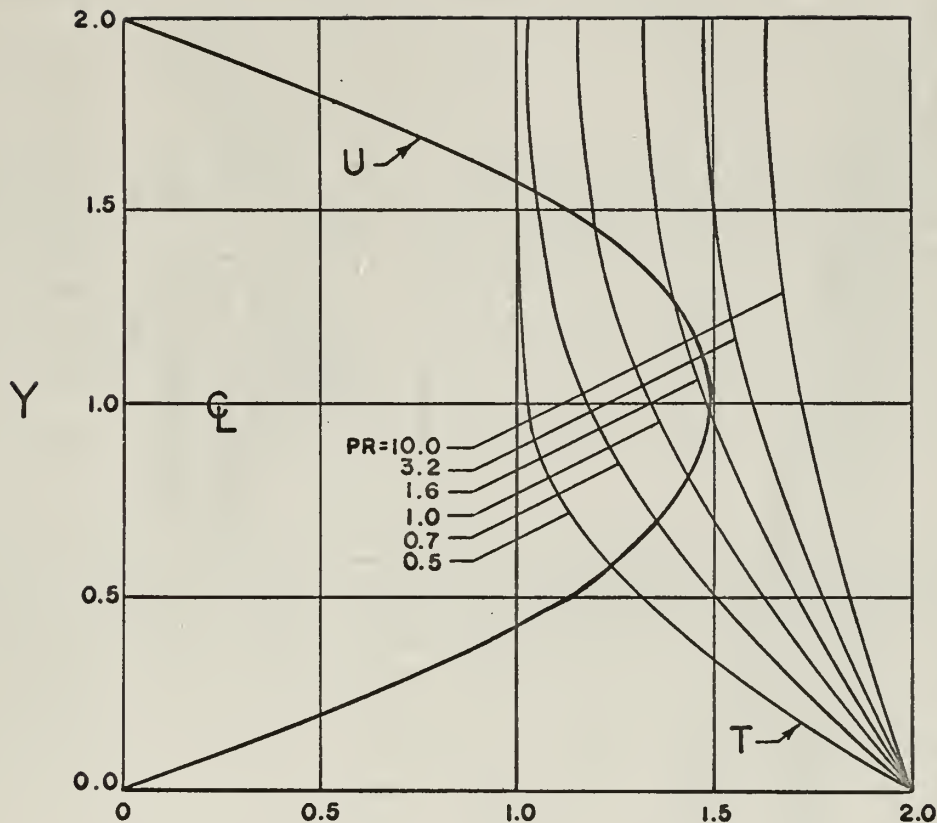
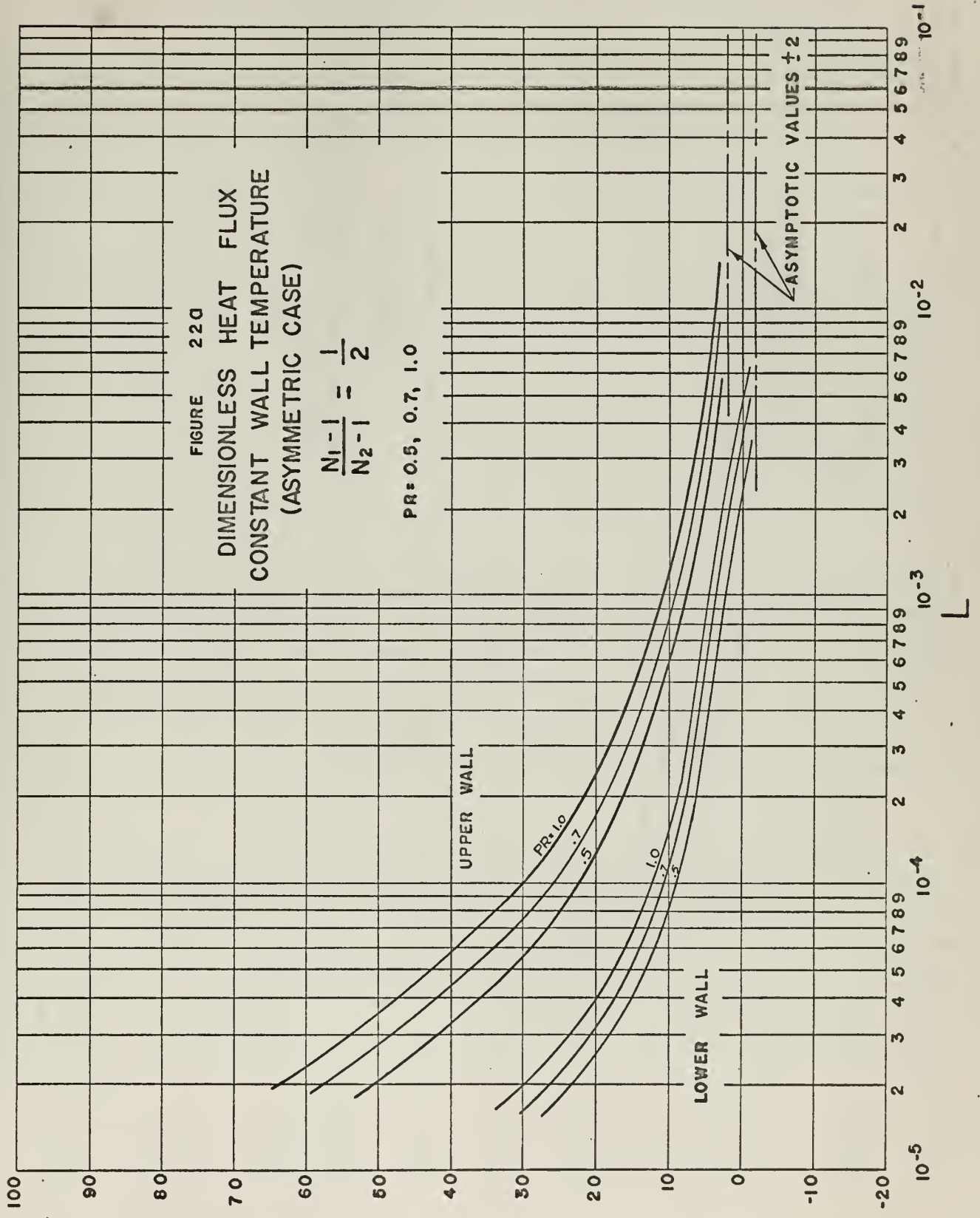
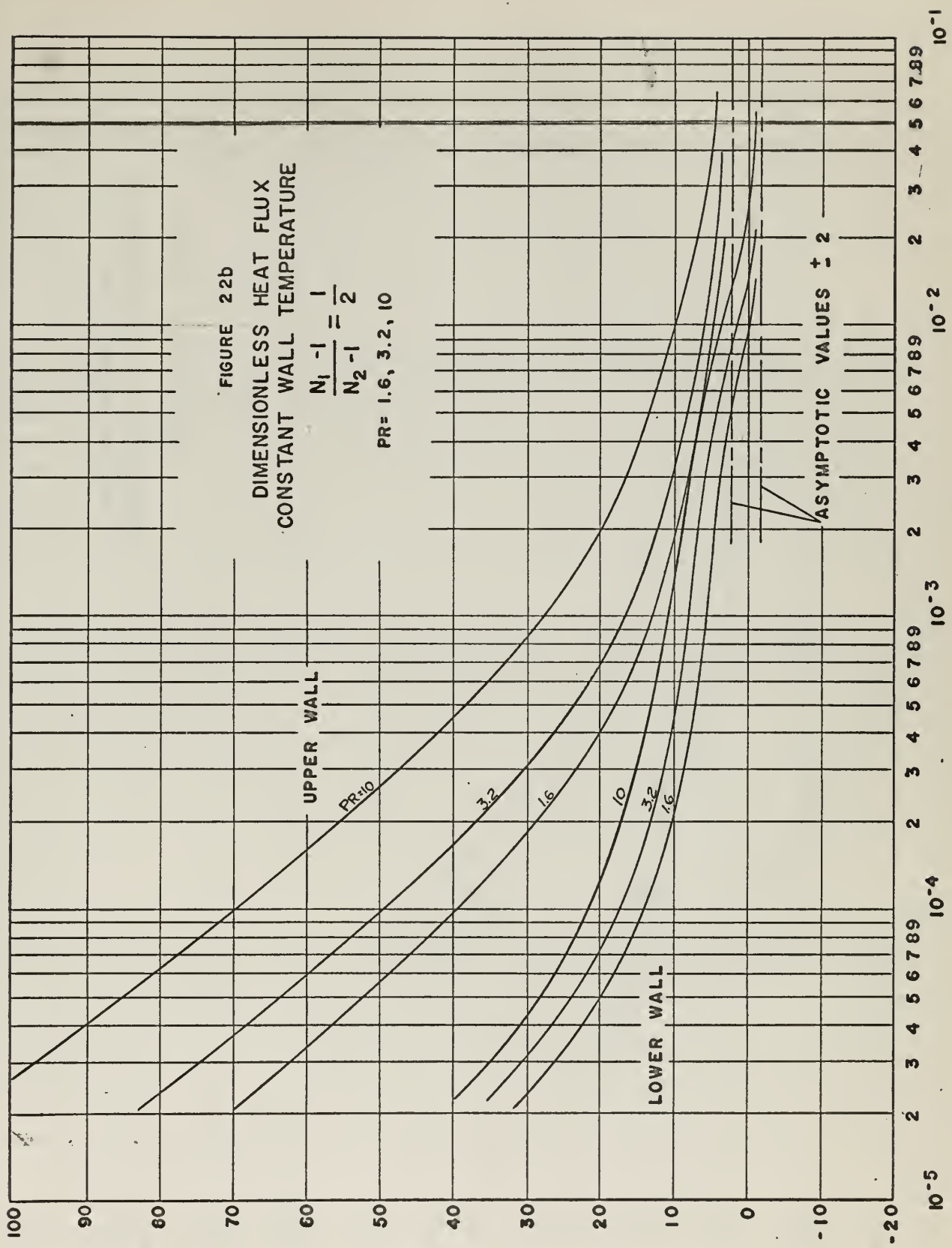
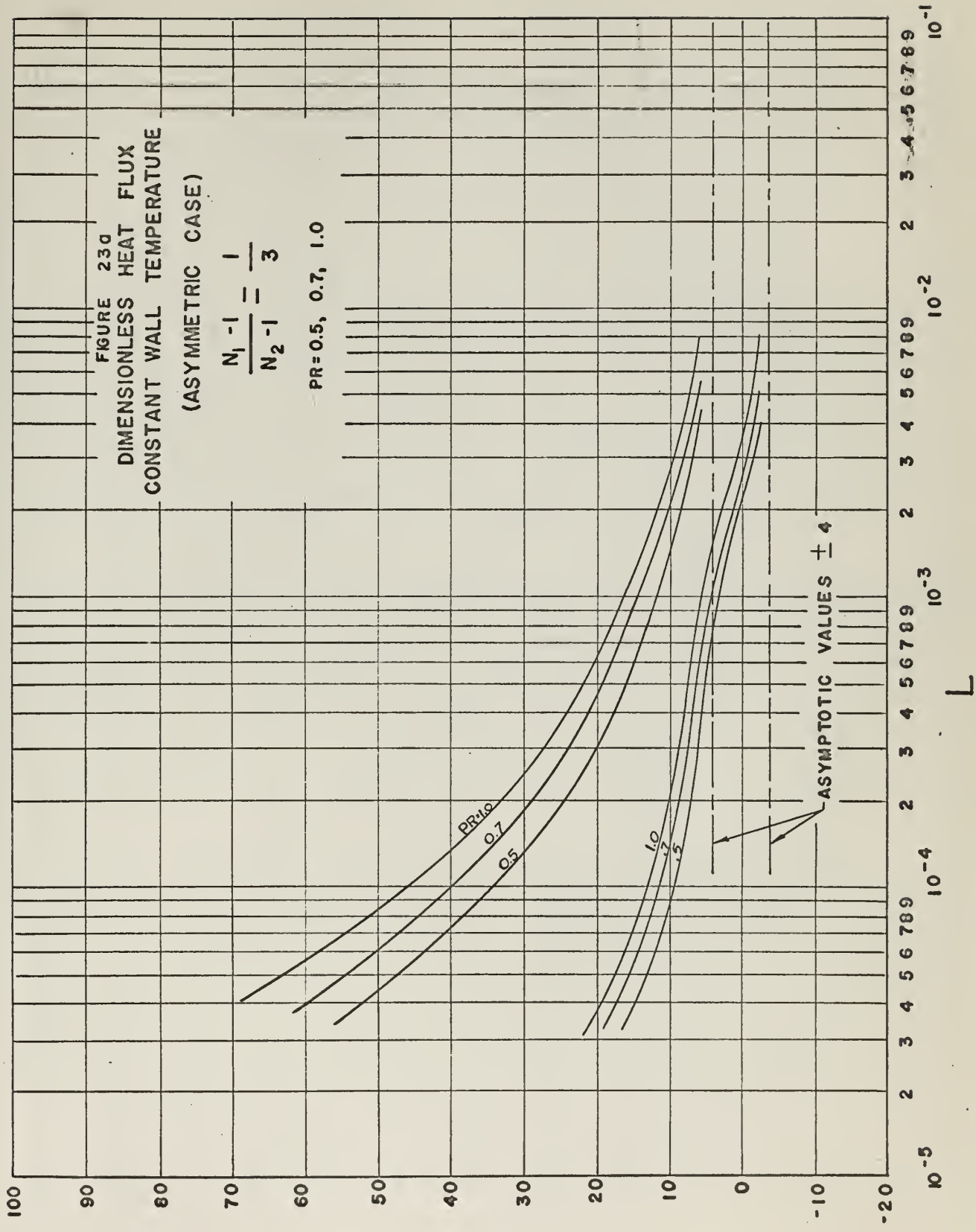


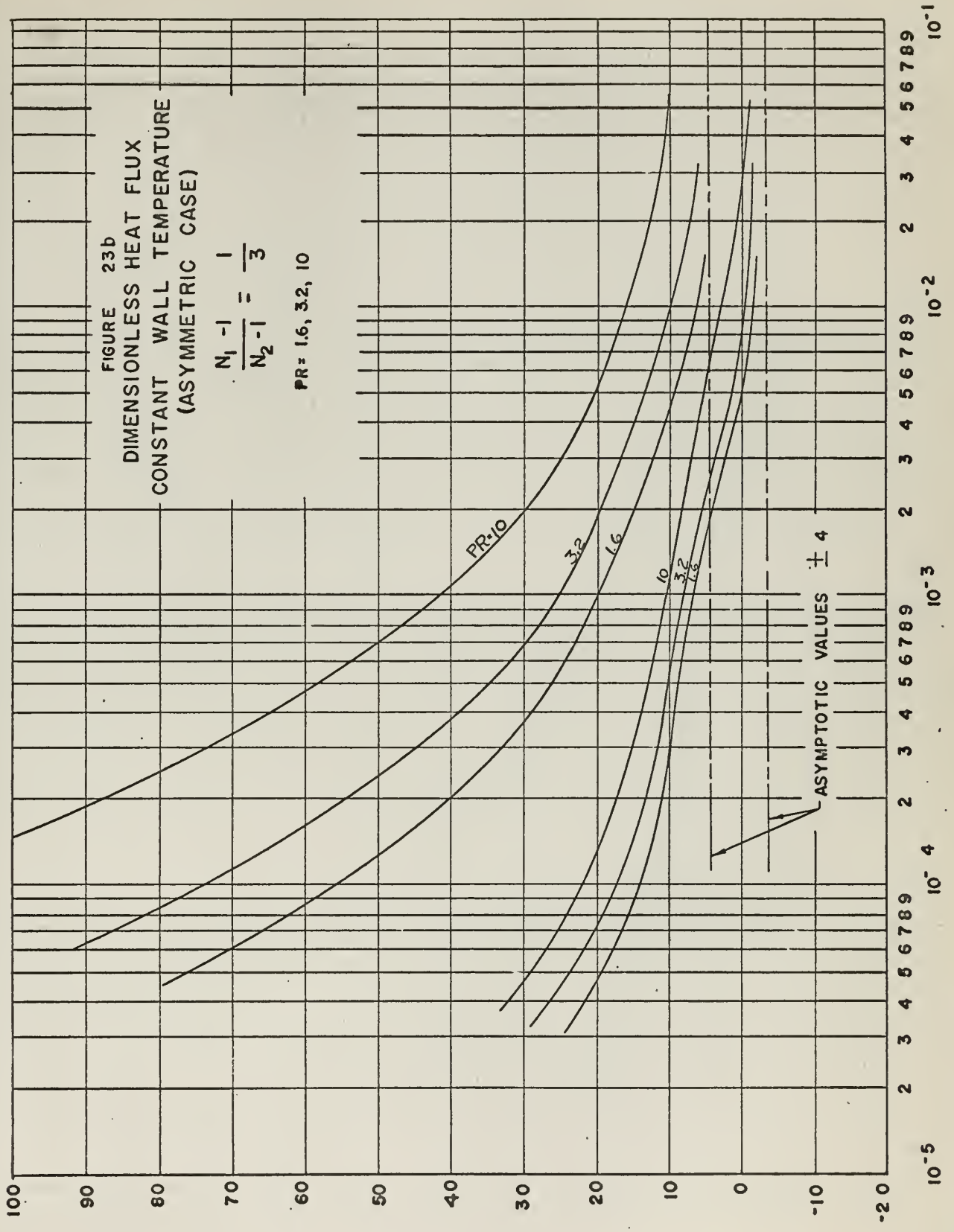
FIGURE 21
TEMPERATURE AND VELOCITY PROFILES
ONE WALL CONSTANT TEMPERATURE
ONE WALL INSULATED
X = 1.00 L = 0.0625

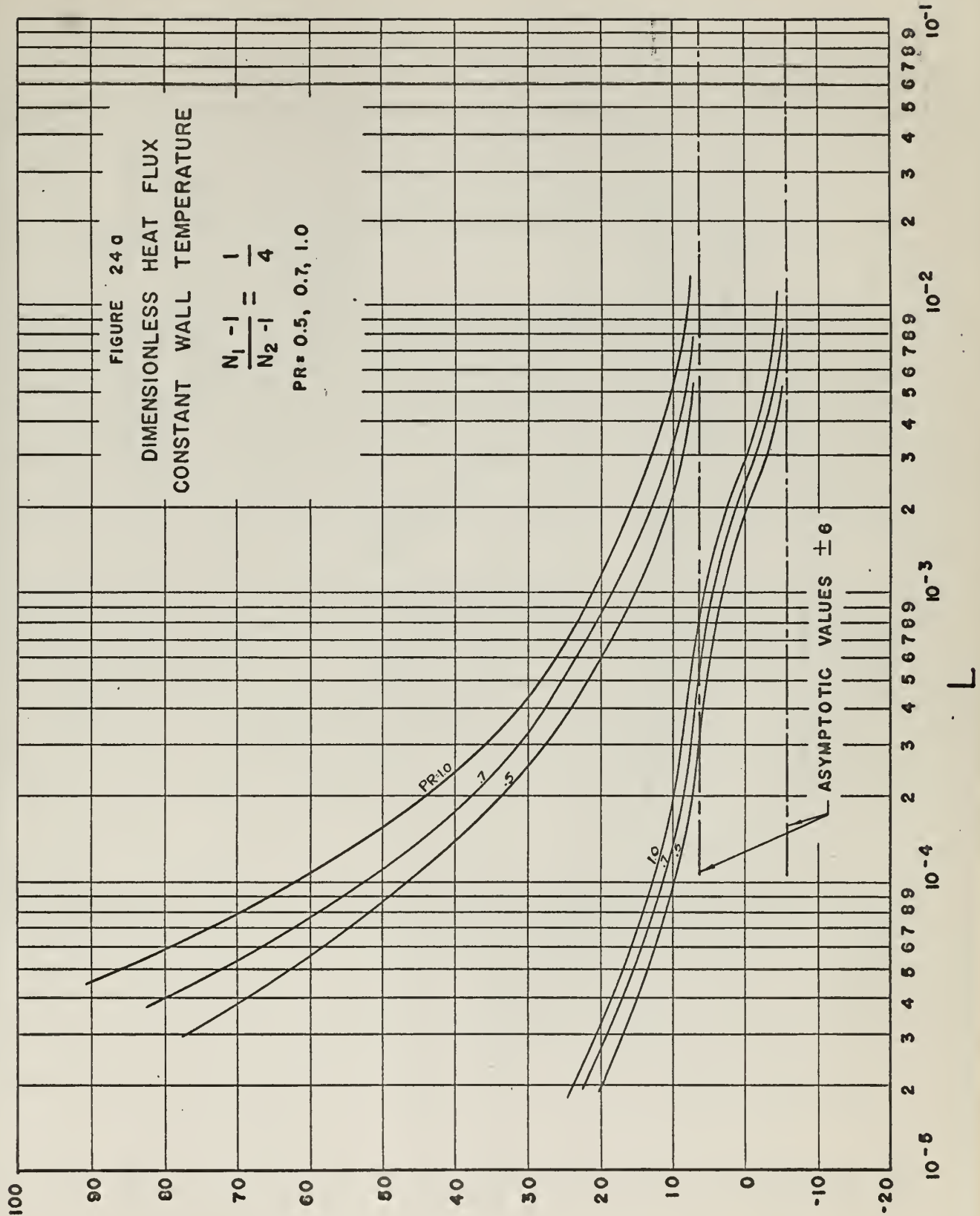


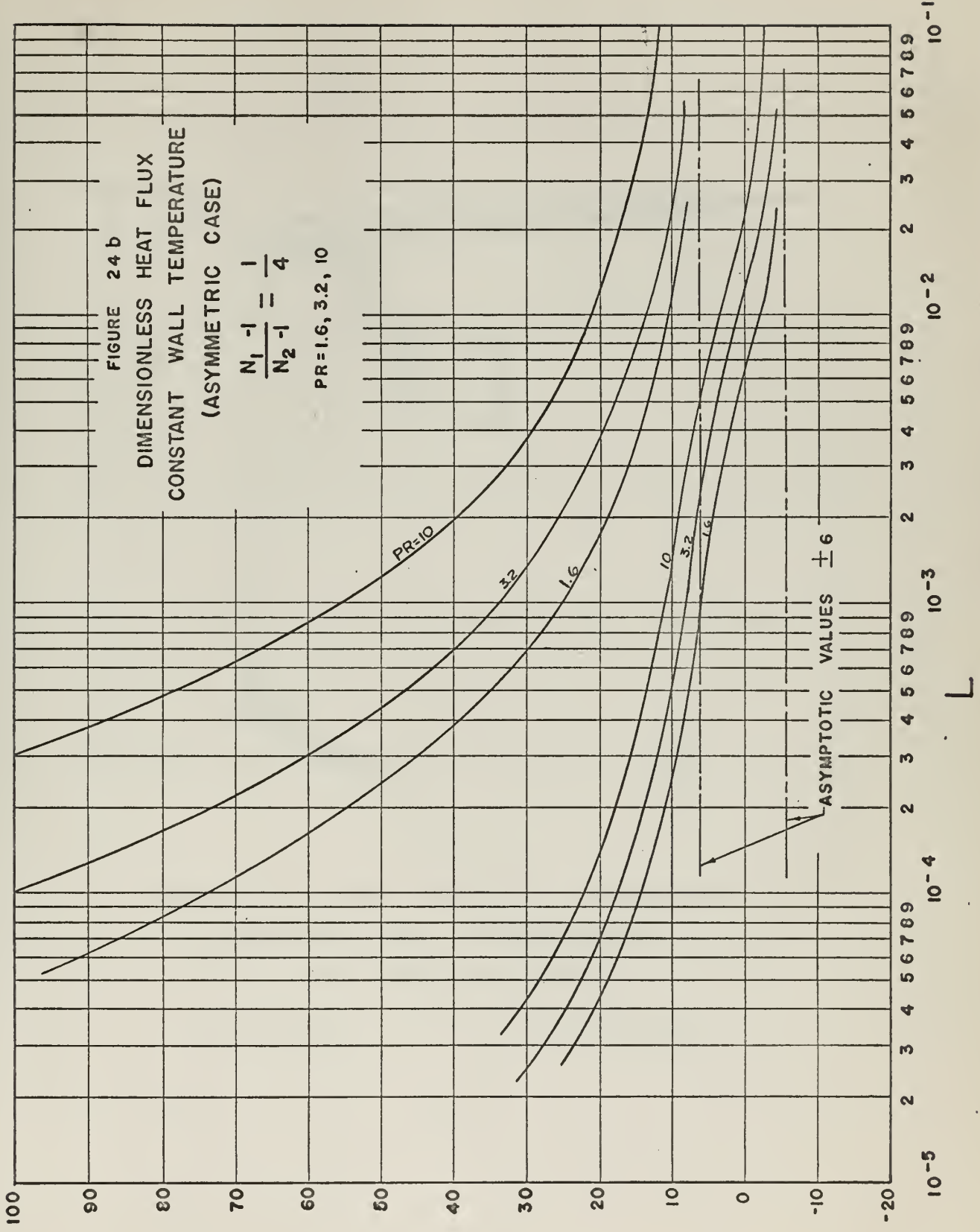












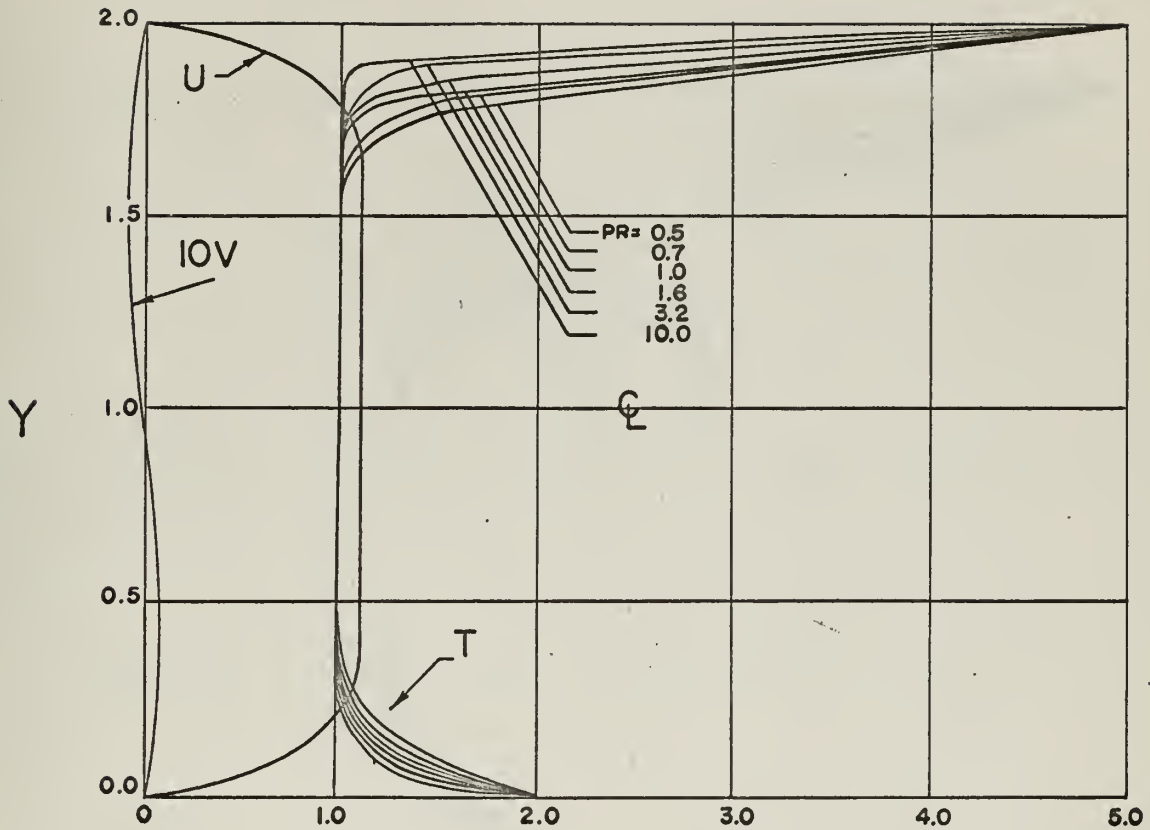


FIGURE 25

TEMPERATURE AND VELOCITY PROFILES
CONSTANT WALL TEMPERATURE
(ASYMMETRIC CASE)

X=0.005

L = 0.0003125

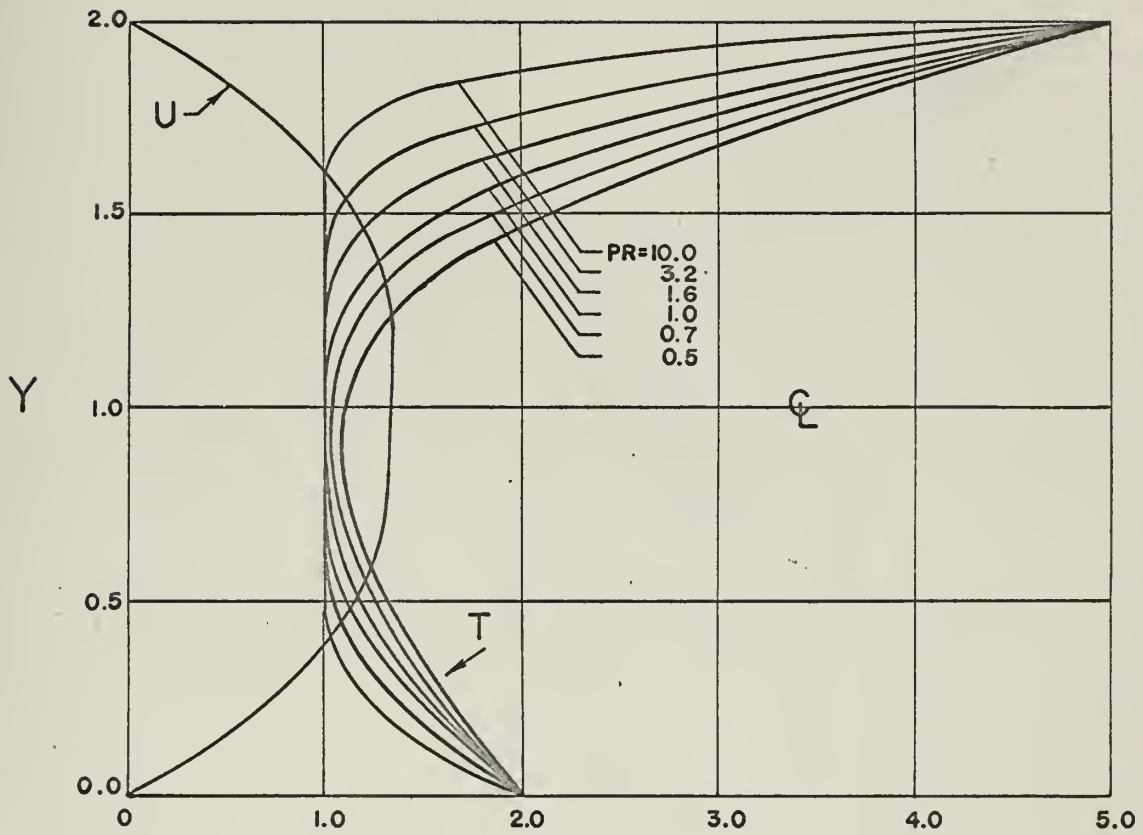


FIGURE 26

TEMPERATURE AND VELOCITY PROFILES
CONSTANT WALL TEMPERATURE
(ASYMMETRIC CASE)

$X = 0.050$

$L = 0.003125$

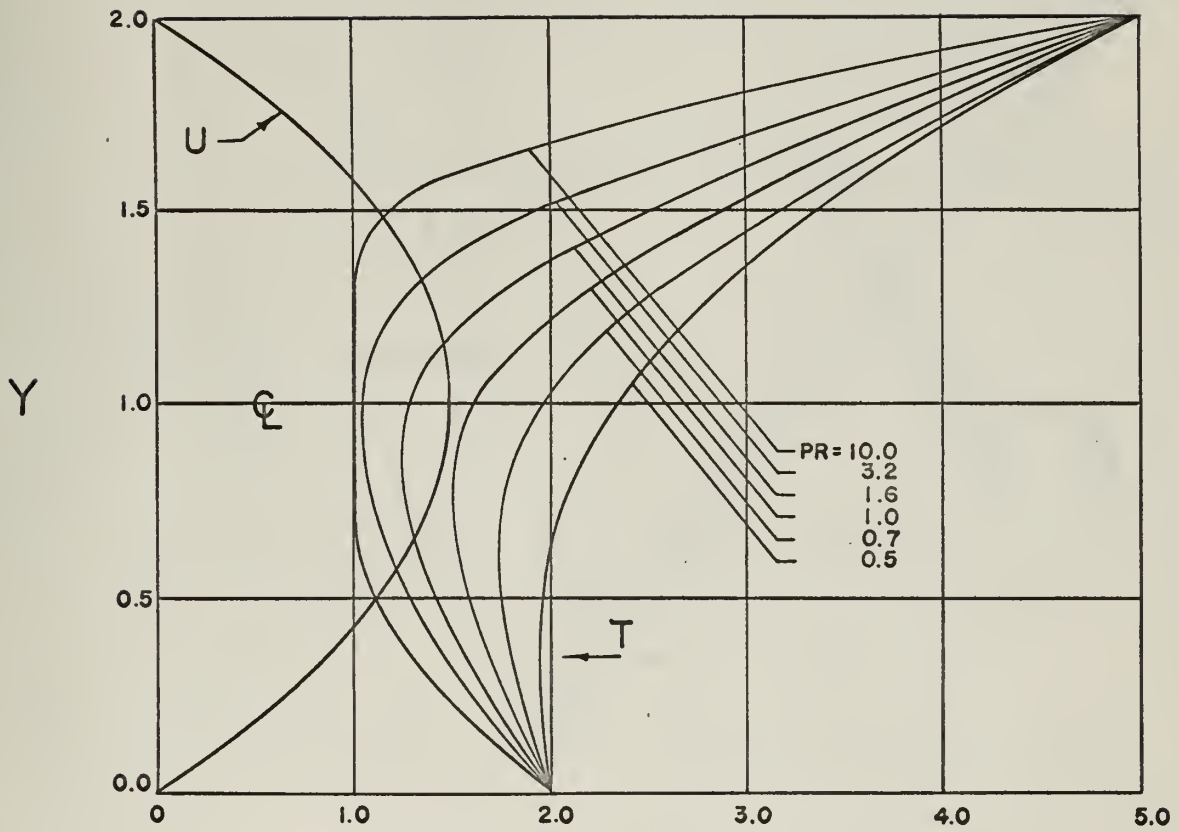


FIGURE 27

TEMPERATURE AND VELOCITY PROFILES
CONSTANT WALL TEMPERATURE
(ASYMMETRIC CASE)

X = 0.250

L = 0.0156

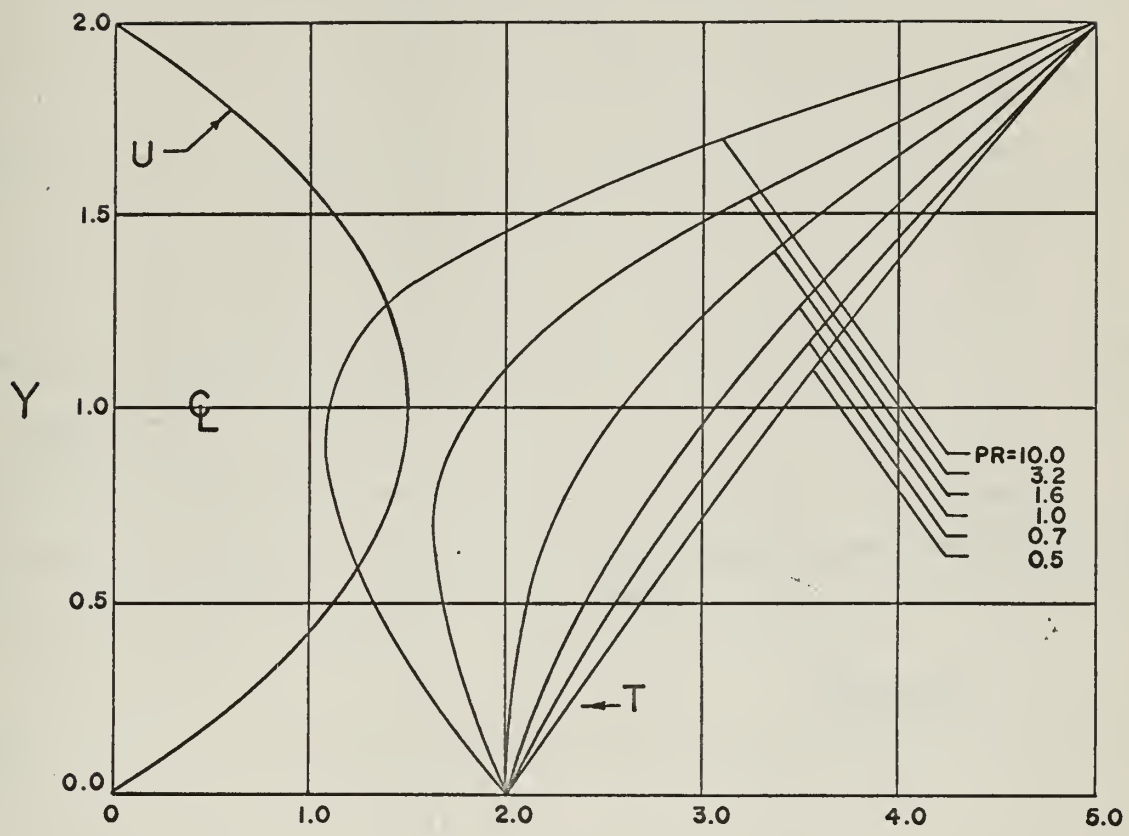


FIGURE 28
TEMPERATURE AND VELOCITY PROFILES
CONSTANT WALL TEMPERATURE
(ASYMMETRIC CASE)

X = 1.00

L = 0.0625

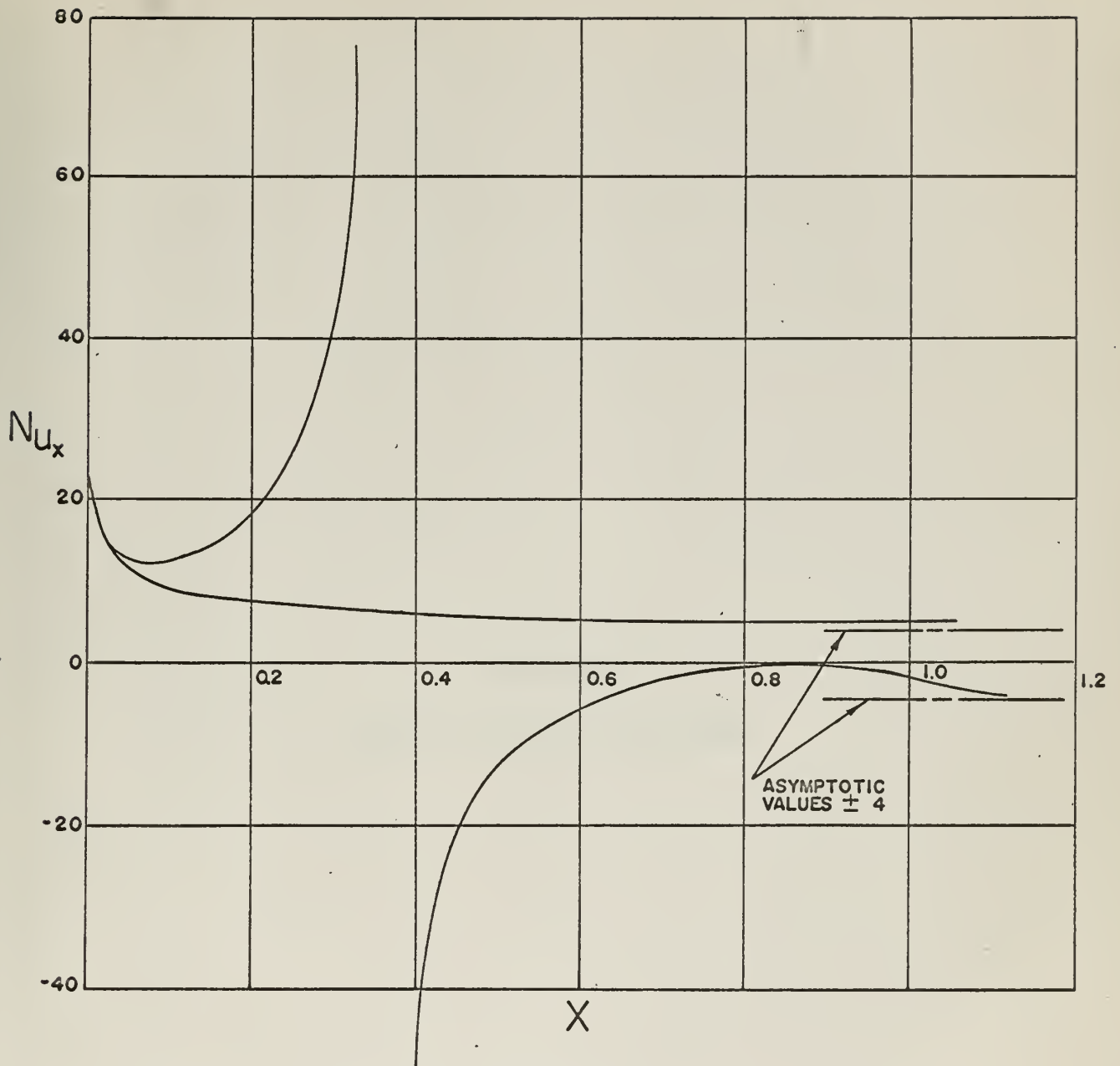


FIGURE 29

LOCAL NUSSLELT NUMBER
 CONSTANT WALL TEMPERATURE
 (ASYMMETRIC CASE)

$$\frac{N_1 - 1}{N_2 - 1} = \frac{1}{4}$$

PR = 0.7

APPENDIX A
SAMPLE FORTRAN 60 PROGRAM


```
..JOB0191F,LUNDBERG
PROGRAM HEATX23
C   CONSTANT HEAT INPUT
C   BODOIA VELOCITY DATA
C   THIS PROGRAM USES A REDUCED GRID OF X=.0001,Y=.05
C   FOR THE FIRST 20 STREAMWISE CALCULATIONS.
C   GRAPH OUTPUTS OF NUSSELT NUMBER VERSUS LENGTH PARAMETER
C   FOR PRANDTL NUMBERS OF 0.5,0.7,1.0,1.6,3.2,AND 10,
C   ARE OBTAINED TO 50 PER CENT OF THE HYDRODYNAMIC
C   DEVELOPMENT. PRINT OUTPUT INCLUDES NUSSELT NUMBER,
C   SOPE OF THE TEMPERATURE PROFILE AT THE WALL , AND THE
C   SLOPE OF THE TEMPERATURE PROFILE AT THE WALL,AND THE MEAN
C   MIXED MEAN TEMPERATURE. IN ADDITION, VELOCITY AND
C   TEMPERATURE VALUES ARE PRINTED AT EACH GRID POINT AT
C   SELECTED STREAMWISE LOCATIONS.
DIMENSION T(30,23),U(30,23),V(30,23),Y(23),X(500)
1,XN(500),ITITLE(12)
READ 500,(ITITLE(I), I=1,6)
READ 500,(ITITLE(I), I=7,12)
500 FORMAT (6A8)
DO 750 KK=1,6
GO TO(40,41,42,43,44,45),KK
40 PR=0.7
GO TO 46
41 PR=0.5
GO TO 888
GO TO 46
42 PR=1.0
GO TO 46
43 PR=1.6
GO TO 46
44 PR=3.2
GO TO 46
45 PR=10.
46 PRINT 523
523 FORMAT (1H1)
PRINT 17, PR
17 FORMAT (//////10X,17H PRANDTL NUMBER =,F5.3)
L=1
GO TO 150
700 READ 701, ((U(I,J), J=13,22), I=2,22)
701 FORMAT (10F6.4)
DO 710 I=2,22
DO 711 J=1,12
711 U(I,J)=U(I,13)
710 CONTINUE
DELX=.0001
DELY=0.05
R=1000.
DO 110 L=2,21
150 UTM=0.0
UM=0.0
XL=L
X(L)=(XL-1.0)*0.0001
```



```
DO 111 J=3,22
XJ=J
Y(L)=(XJ-3.0)*0.05
Y(23)=1.0
U(1,J)=1.
U(1,23)=1.0
V(1,J-1)=0.0
V(1,J)=0.
T(1,J)=1.0
T(1,J+1)=1.0
T(1,J-1)=1.0
T(L,1)=T(L,5)
U(L,1)=U(L,5)
U(L,23)=0.0
U(L,2)=U(L,4)
V(L,3)=0.0
V(L,2)=V(L,4)
C THERMAL BOUNDARY CONDITIONS
T(L,23)=T(L,22)+.05
T(L,2)=T(L,4)
IF(L-1) 109,109,108
108 V(L,J)= V(L,J-1) + DELY/(2.*DELX*R) * (U(L-1,J)-U(L+1,J))
109 A= DELX/ (U(L,J)*PR*DELY**2)
V(L,23)=0.0
B= (DELX*R*V(L,J)) / (2.*DELY*U(L,J))
T(L+1,J)=(A-B)*T(L,J+1)+(1.-2.*A)*T(L,J)+(A+B)*T(L,J-1)
IF(J-3) 113,113,112
113 UTM=UTM+.5*U(L,J)*T(L,J)
UM=UM+.5*U(L,J)
GO TO 114
112 UTM=UTM+U(L,J)*T(L,J)
UM=UM+U(L,J)
114 TM=UTM/UM
111 CONTINUE
T1= ( T(L,23)-T(L,22)) / DELY
T2= T(L,23) - TM
XN(L)=4.0*T1/T2
131 PRINT 118, X(L),XN(L),T2,T1,TM
118 FORMAT (// 4H X =,F6.4,5X,14H NUSSELT NO. =,F8.5,5X,8H TW-TM =,
1F8.5,5X,8H SLOPE =,F8.5,5X,5H TM =,F8.5)
PRINT119, (T(L,J), J=1,12)
PRINT119, (T(L,J), J=13,23)
119 FORMAT (/9H TEMP. =,12F7.4)
PRINT120, (U(L,J), J=1,12)
PRINT120, (U(L,J), J=13,23)
120 FORMAT (/ 9H X VEL. =,12F7.4)
PRINT121, (V(L,J), J=1,12)
PRINT121, (V(L,J), J=13,23)
121 FORMAT (/ 9H Y VEL. =,12F7.4)
IF(L-1) 700,700,110
110 CONTINUE
CALL DRAW (21,X,XN,MOD,0,LAB,ITITLE,.04,10.,0,0,0,0,6, 6,1, LAST)
DO 720 N=2,11
M=2*N-1
```



```
U(1,N)=U(11,M)
U(2,N)=U(21,M)
T(2,N)=T(21,M)
PRINT 771, M, U(2,N),T(2,N)
771 FORMAT (I10,2F10.5)
720 CONTINUE
85 L=2
DO 10 M=2,250
70 XM=M
Y=0.0
DELY=0.1
DELX=0.001
X(M)=DELX*XM
I=L+1
N3N=M
N=L+1
82 IF(M- 99) 72,73,73
72 READ 1 (U(I,11),U(I,10),U(I,9),U(I,8),U(I,7),U(I,6)
1,U(I,5),U(I,4),U(I,3),U(I,2) )
1 FORMAT (10F6.4)
73 IF(M-99 ) 50,51,52
52 IF(M-149) 51,53,54
54 IF(M-199) 53,55,55
51 UU=XM- 99.
U(N,2) =1.4388+.000740*UU
U(N,3) =1.4292+.000674*UU
U(N,4) =1.3993+.000492*UU
U(N,5) =1.3454+.000238*UU
U(N,6) =1.2628-.000034*UU
U(N,7) =1.1467-.000262*UU
U(N,8) = .9938-.000410*UU
U(N,9) = .8022-.000452*UU
U(N,10)= .5720-.000388*UU
U(N,11)= .3042-.000230*UU
GO TO 50
53 UU=XM-149.
U(N,2) =1.4758+.000290*UU
U(N,3) =1.4629+.000266*UU
U(N,4) =1.4239+.000194*UU
U(N,5) =1.3573+.000092*UU
U(N,6) =1.2611-.000014*UU
U(N,7) =1.1336-.000104*UU
U(N,8) = .9733-.000160*UU
U(N,9) = .7796-.000176*UU
U(N,10)= .5526-.000150*UU
U(N,11)= .2926-.000092*UU
GO TO 50
55 UU=XM-199.
U(N,2) =1.4903+.0000121*UU
U(N,3) =1.4762+.0000110*UU
U(N,4) =1.4336+.0000080*UU
U(N,5) =1.3619+.0000026*UU
U(N,6) =1.2604-.0000005*UU
U(N,7) =1.1284-.0000042*UU
```



```

U(N,8) = .9653-.0000066*UU
U(N,9) = .7708-.0000072*UU
U(N,10) = .5451-.0000063*UU
U(N,11) = .2880-.0000475*UU
50 UTM=0.0
   UM=0.0
   DO 11 J=2,11
     XJ=J
     Y(J)=DELY*XJ-.2
     U(L,12)=0.0
     V(L,2)=0.0
     V(L,1)=V(I,3)
     Y(12)=1.0
     T(L,12)=T(L,11)+0.1
     T(L,1)=T(L,3)
     U(L,1)=U(L,3)
8   V(L,J)= V(L,J-1) + DELY/(2.*DELX*R) * (U(L-1,J)-U(L+1,J))
   A= DELX/ (U(L,J)*PR*DELY**2)
   V(L,12)=0.0
   B= (DELX*R*V(L,J)) / (2.*DELY*U(L,J))
   T(L+1,J)=(A-B)*T(L,J+1)+(1.-2.*A)*T(L,J)+(A+B)*T(L,J-1)
   IF(J-2) 13,13,12
13  UTM=UTM+.5*U(L,J)*T(L,J)
   UM=UM+.5*U(L,J)
   GO TO 14
12  UTM=UTM+U(L,J)*T(L,J)
   UM=UM+U(L,J)
14  TM=UTM/UM
11  CONTINUE
   T1= ( T(L,12)-T(L,11) ) / DELY
   T2= T(L,12)-TM
   XN(M)=4.0*T1/T2
   IF(N3N-50 ) 31,31,30
30  IF((N3N/25)*25-N3N) 15,31,31
31  PRINT 18,X(M),XN(M),T2,T1,TM
18  FORMAT (// 4H X =,F8.3,5X,14H NUSSELT NO. =,F8.5,5X,8H TW-TM =,
19  F8.5,5X,8H SLOPE =,F8.5,5X,5H TM =,F8.5)
   PRINT 19, (T(L,J), J=1,12)
19  FORMAT (/9H TEMP. =,12F7.4)
   PRINT 20, (U(L,J), J=1,12)
20  FORMAT (/ 9H X VEL. =,12F7.4)
   PRINT 21, (V(L,J), J=1,12)
21  FORMAT (/ 9H Y VEL. =,12F7.4)
15  DO 60 J=2,11
     T(L,J)=T(L+1,J)
     U(L-1,J)=U(L,J)
60  U(L,J)=U(L+1,J)
10  CONTINUE
   IF(KK-6) 760,761,761
761 MOD=3
C   GO TO 762
760 MOD=2
C 762 CALL DRAW(497,X,XN,MOD,0,LAB,ITITLE,.04,10.,0,0,0,0,6, 6,1,LAST).
750 CONTINUE

```


UDLEY KNOX LIBRARY
NAVAL POSTGRADUATE SCHOOL
MONTEREY CA 93943-5101

THIS DOCUMENT PROVIDED BY THE ABBOTT AEROSPACE
DUDLEY KNOX LIBRARY
TECHNICAL LIBRARY
ABBOTTAEROSPACE.COM

3 2768 00019083 9